JOC The Journal of Organic Chemistry

Article

pubs.acs.org/joc

# Synthesis and Characterization of Oligodeoxyribonucleotides Modified with 2′-Amino-α-L-LNA Adenine Monomers: High-Affinity Targeting of Single-Stranded DNA

Nicolai K. Andersen,[†,§] Brooke A. Anderson,[‡,§] Jesper Wengel,[†] and Patrick J. Hrdlicka[‡,*]

[†]Nucleic Acid Center, Department of Physics, Chemistry and Pharmacy, University of Southern Denmark, 5230 Odense, Denmark

[‡]Department of Chemistry, University of Idaho, Moscow, Idaho 83844-2343, United States

Supporting Information

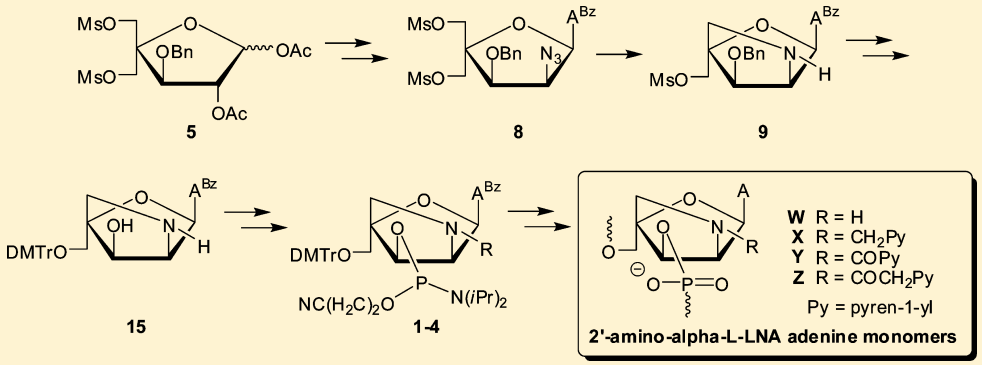


**ABSTRACT:** The development of conformationally restricted nucleotide building blocks continues to attract considerable interest because of their successful use within antisense, antigene, and other gene-targeting strategies. Locked nucleic acid (LNA) and its diastereomer α-L-LNA are two interesting examples thereof. Oligonucleotides modified with these units display greatly increased affinity toward nucleic acid targets, improved binding specificity, and enhanced enzymatic stability relative to unmodified strands. Here we present the synthesis and biophysical characterization of oligodeoxyribonucleotides (ONs) modified with 2′-amino-α-L-LNA adenine monomers **W**–**Z**. The synthesis of the target phosphoramidites **1**–**4** is initiated from pentafuranose **5**, which upon Vorbrüggen glycosylation, O2′-deacylation, O2′-activation and C2′-azide introduction yields nucleoside **8**. A one-pot tandem Staudinger/intramolecular nucleophilic substitution converts **8** into 2′-amino-α-L-LNA adenine intermediate **9**, which after a series of nontrivial protecting-group manipulations affords key intermediate **15**. Subsequent chemoselective N2′-functionalization and O3′-phosphitylation give targets **1**–**4** in ∼1–3% overall yield over 11 steps from **5**. ONs modified with pyrene-functionalized 2′-amino-α-L-LNA adenine monomers **X**–**Z** display greatly increased affinity toward DNA targets ($\Delta T_m$/modification up to +14 °C). Results from absorption and fluorescence spectroscopy suggest that the duplex stabilization is a result of pyrene intercalation. These characteristics render N2′-pyrene-functionalized 2′-amino-α-L-LNAs of considerable interest for DNA-targeting applications.

## INTRODUCTION

Major efforts have been devoted over the past 20 years to the development of conformationally restricted nucleotides. Oligonucleotides that are modified with these building blocks often display markedly increased affinity toward nucleic acid targets, improved discrimination of nontargets, and greater resistance against enzymatic degradation relative to reference strands.[1] Such oligonucleotides are accordingly widely used for nucleic acid-targeting applications in molecular biology, biotechnology, and medicinal chemistry.[2] Locked nucleic acid (LNA) is one of the most prominent members of this compound class because of its extraordinary affinity toward DNA and RNA complements (Figure 1); thus, increases in the thermal denaturation temperature ($T_m$) of up to +10 °C per modification have been observed.[3−5] The diastereomeric α-L-LNA (Figure 1) shares many characteristics with LNA, including very high affinity toward DNA/RNA targets, but is less well characterized as a result of its more limited commercial availability.[6] The interesting properties of LNA, α-L-LNA, and other conformationally restricted nucleotides have spurred the development of many analogues.[1,7]

As part of our ongoing interest in LNA chemistry and diagnostic applications of pyrene-functionalized oligonucleotides,[2c,8] we recently pursued the development of N2′-pyrene-functionalized 2′-amino-α-L-LNA thymine monomers (Figure 1).[9] Oligodeoxyribonucleotides (ONs) modified with these monomers display remarkable affinity toward complementary DNA, as the pyrene moieties are preorganized to intercalate and engage in stacking with neighboring nucleobases upon

**Received:** October 13, 2013
**Published:** December 4, 2013

  

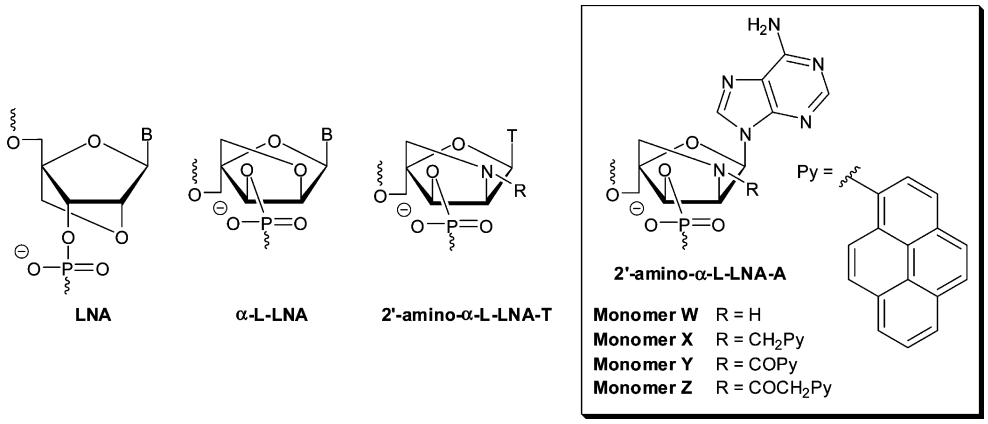


**Figure 1.** Structures of LNA, α-L-LNA, and the 2′-amino-α-L-LNA monomers studied herein. T = thymin-1-yl.

**Scheme 1. Retrosynthetic Analysis of 2′-Amino-α-L-LNA-adenine Monomers W–Z**[a]

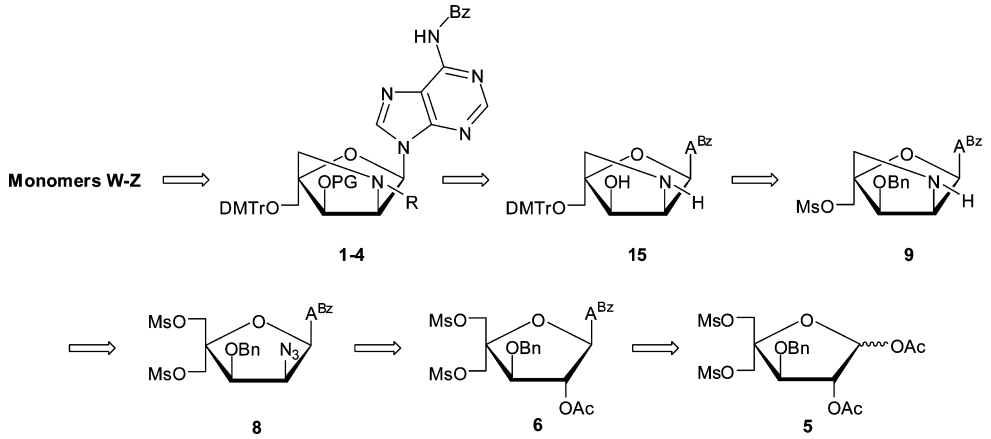


[a]Abbreviations: PG = PN(*i*Pr)$_2$OCH$_2$CH$_2$CN; R = H, CH$_2$Py, COPy, and COCH$_2$Py for **W–Z**, respectively; py = pyren-1-yl; A$^{Bz}$ = 6-*N*-benzoyladenin-9-yl.

duplex formation.[9b] Thus, increases in $T_m$ of up to 20 °C per modification have been observed for short ONs modified with these building blocks. We have taken advantage of these characteristics and have developed probes for a variety of diagnostic applications. For example, ONs modified with two next-nearest-neighbor incorporations of 2′-*N*-(pyren-1-yl)-acetyl-2′-amino-α-L-LNA-T monomers are promising tools for the detection of single-nucleotide polymorphisms, which are the most prevalent type of genetic mutation in the human genome.[10] These probes efficiently discriminate between complementary and single-base-mismatched DNA/RNA targets through differences in pyrene excimer emission levels. In another example, the fluorescence of ONs modified with 2′-*N*-(pyren-1-yl)acetyl-2′-amino-α-L-LNA-T monomers was found to increase 16-fold upon hybridization with DNA targets featuring abasic sites (i.e., DNA lesions that result in genomic mutations and emergence of cancers if unrepaired).[11] We have also utilized N2′-pyrene-functionalized 2′-amino-α-L-LNA-T monomers as the key activating components of the so-called Invader probes, which recognize mixed-sequence double-stranded DNA.[12] Unfortunately, the synthesis of N2′-pyrene-functionalized 2′-amino-α-L-LNA-thymine phosphoramidites is challenging (~20 steps, <4% overall yield from diacetone-α-D-glucose), mainly because of unsuccessful attempts to introduce the necessary C2′-azido group at the nucleoside level without concomitant O2,O2′-anhydronucleoside formation.[9a] This forced us to introduce the azido group at the carbohydrate level, which resulted in a loss of anchimeric assistance from the O2-position during Vorbrüggen glycosylation and the formation of anomeric nucleoside mixtures. We hypothesized that these synthetic difficulties might be overcome with the corresponding adenine derivates, as the formation of anhydronucleosides would be unlikely. Easier access to N2′-pyrene-functionalized 2′-amino-α-L-LNA monomers is desirable in order to evaluate the diagnostic potential of these building blocks in greater detail.

In the present article, we report the synthesis and characterization of ONs modified with four different 2′-amino-α-L-LNA-adenine monomers **W–Z** (Figure 1). The ONs were characterized via thermal denaturation, UV–vis, and fluorescence experiments and shown to display extraordinary thermal affinity toward complementary DNA ($\Delta T_m$/modification up to 14.0 °C) and photophysical characteristics consistent with intercalative binding modes for the pyrene moieties.[13]

## RESULTS AND DISCUSSION

**Retrosynthetic Analysis of 2′-Amino-α-L-LNA-A Monomers.** Inspired by our previously reported synthesis of the corresponding thymine monomers,[9] we identified adenine derivative **15** as a suitable substrate for chemoselective N2′-functionalization and subsequent O3′-phosphitylation, which were expected to yield the target 6-*N*-benzoyladenin-9-yl


dx.doi.org/10.1021/jo4022937 | J. Org. Chem. 2013, 78, 12690–12702

**Scheme 2. Synthesis of Intermediate 9**[a]

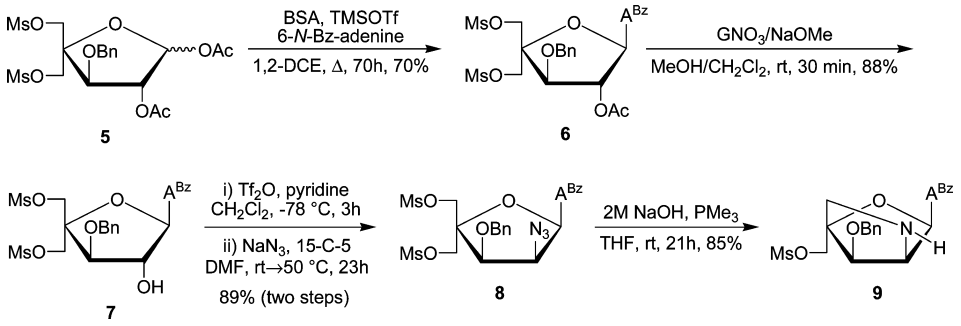


[a]Abbreviations: BSA = *N*,*O*-bis(trimethylsilyl)acetamide; 1,2-DCE = 1,2-dichloroethane; $A^{Bz}$ = 6-*N*-benzoyladenin-9-yl; $GNO_3$ = guanidinium nitrate; 15-C-5: 15-crown-5.

**Scheme 3. Synthesis of Key Intermediate 15**[a]

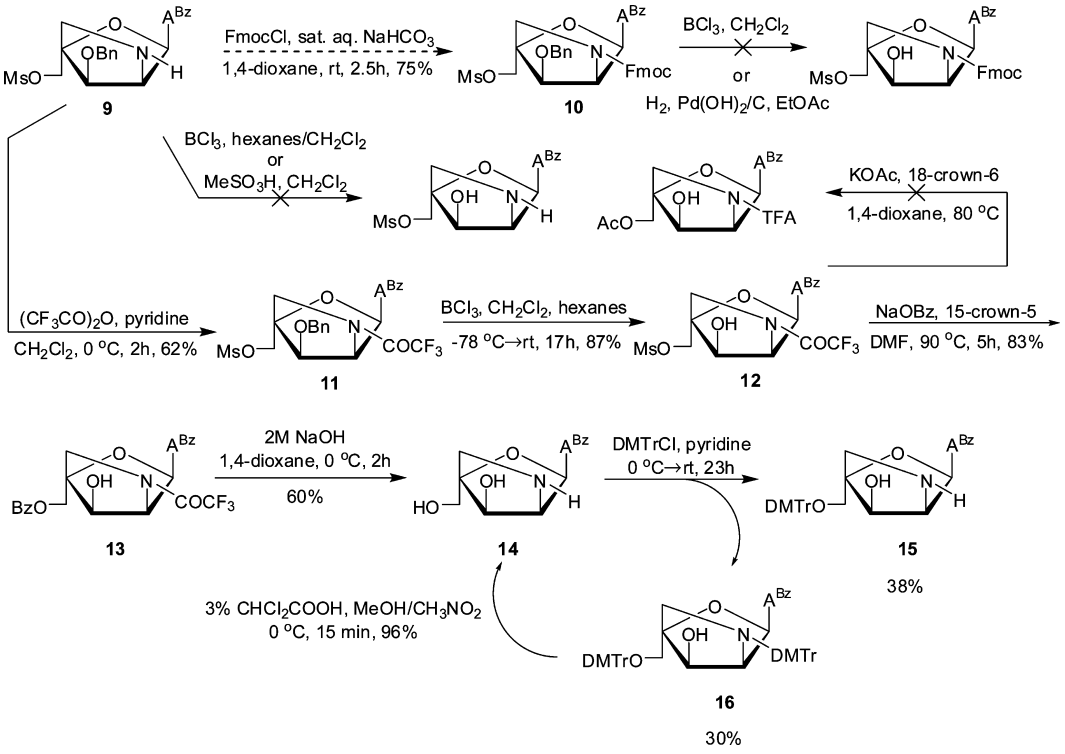


[a]Abbreviations: $A^{Bz}$ = 6-*N*-benzoyladenin-9-yl; DMTr = 4,4′-dimethoxytrityl; FmocCl = 9′-fluorenylmethyl chloroformate.

nucleosides **1**–**4** (Scheme 1). We surmised that key intermediate **15** could be obtained from nucleoside **9** via a series of protecting-group manipulations. The O3′-benzyl group was selected because of (i) its stability under acidic and basic reaction conditions, allowing it to be introduced at the beginning of the synthetic route, and (ii) its ability to be removed under conditions that have only a minimal effect on the 6-*N*-benzoyl group of adenine.[14] We expected to construct the 2-oxo-5-azabicyclo[2.2.1]heptane skeleton of **9** in a manner similar to that originally reported for 2′-amino-*β*-D-LNA,[15] namely, via a one-pot tandem Staudinger/intramolecular nucleophilic substitution reaction, which revealed nucleoside **8** as an early target. In contrast to our synthesis of the corresponding thymine monomer, where the C2′-azido group had to be introduced at the carbohydrate stage,[9a] we decided to introduce the 2′-azido group of **8** at the nucleoside stage, anticipating that selective O2′-deacylation of known nucleoside **6**[6b] and subsequent O2′-activation and introduction of the azido group would provide **8**. Importantly, the anchimeric assistance provided by the O2-substituent during the Vorbrüggen glycosylation of **5** to give **6** prevents formation of anomeric mixtures, which is one of the drawbacks in the synthesis of 2′-amino-*α*-L-LNA-T monomers.[9a]

**Synthesis of Key Intermediate 15.** Fully protected pentafuranose **5**, which was obtained from diacetone-*α*-D-glucose in six steps and ∼30% overall yield,[6b,16] served as the starting material for the synthesis of key intermediate **15** (Scheme 2). Glycosyl donor **5** was converted into alcohol **7** following protocols that deviated from the known route[6b] in the following manner: (i) the use of trimethylsilyl triflate as the Lewis acid and 1,2-dichloroethane as the reaction solvent during Vorbrüggen glycosylation of **5** afforded **6** in higher yield and with easier workup than the original protocol involving tin(IV) chloride and acetonitrile (70% vs 57%, respectively);


dx.doi.org/10.1021/jo4022937 | J. Org. Chem. 2013, 78, 12690−12702

(ii) the use of the guanidinium nitrate/sodium methoxide reagent mixture[17] resulted in slightly more efficient O2′-deacylation of **6** than the original protocol enploying dilute methanolic ammonia (88% vs 79% yield), although the dilute reaction conditions of the former approach rendered it less practical for large-scale reactions. Alcohol **7** was O2′-triflated and treated with sodium azide and 15-crown-5 in DMF at elevated temperatures to furnish azide **8** in excellent yield (89% over two steps). IR spectra of **8** verified the presence of the azide group (sharp band at 2115 $cm^{-1}$). Nucleoside **8** was converted into the desired 2′-amino-α-L-LNA intermediate **9** via a one-pot tandem Staudinger/intramolecular nucleophilic substitution reaction using alkaline trimethylphosphine[15] in a satisfying 85% yield.[18] The 2-oxo-5-azabicyclo[2.2.1]heptane skeleton and stereochemical configuration of **9** were verified by NOE difference experiments on downstream products (vide infra).

The protecting-group manipulations needed to convert nucleoside **9** into key intermediate **15** proved to be surprisingly challenging (Scheme 3). For example, O3′-debenzylation of bicyclic nucleoside **9** was unsuccessful using boron trichloride or methanesulfonic acid in dichloromethane. Similarly, the corresponding N2′-Fmoc-protected nucleoside **10** (obtained by reacting **9** with 9′-fluorenylmethyl chloroformate under Schotten–Baumann conditions; results not shown) failed to undergo O3′-debenzylation with $BCl_3$ in dichloromethane or by standard hydrogenolysis. Additional attempted strategies are outlined in Scheme S1 in the Supporting Information. Therefore, it proved necessary to protect the N2′-position of bicyclic nucleoside **9** as a trifluoroacetamide to give nucleoside **11** in 62% yield, which was then O3′-debenzylated with $BCl_3$ in hexanes to give nucleoside **12** in 87% yield (Scheme 3). Protection of the O3′-position as a napthyl ether would be an attractive alternative option, as it can be cleaved using DDQ,[7a] but this option was not considered at the time of the synthesis. Subsequent nucleophilic substitution of the C5′-mesylate group of **12** was attempted using potassium acetate and 18-crown-6, but this resulted in the formation of numerous side products according to analytical TLC, and the approach was abandoned (Scheme 3). Instead, treatment of **12** with sodium benzoate and 15-crown-5 in hot DMF afforded O5′-benzoylated nucleoside **13** in 83% yield. Subsequent treatment of nucleoside **13** with aqueous sodium hydroxide in 1,4-dioxane effected the cleavage of both the O5′-benzoyl and N2′-trifluoroacetamide protecting groups, affording polar amino alcohol **14** in 60% yield after column chromatography. The O5′-hydroxyl group of nucleoside **14** was subsequently protected as the 4,4′-dimethoxytrityl (DMTr) ether using standard conditions to afford key intermediate **15**. Curiously, the reaction proceeded in no more than 38% yield, as significant amounts of N2′,O5′-di-DMTr-protected nucleoside **16** were produced as well (30% yield). Efforts to optimize the yield of **15** (e.g., slow addition of DMTr-Cl at low temperatures) were unsuccessful. However, it was possible to recycle nucleoside **16** into amino diol **14** using 3% dichloroacetic acid in a mixture of methanol and nitromethane[19] in up to 96% yield. An alternative strategy toward **15**, involving N2′-Fmoc protection of **14** and subsequent O5′-DMTr-protection and N2′-Fmoc deprotection, was dismissed because O5′-DMTr protection was inefficient (~40% yield; results not shown). Thus, the preferred route (**5** →→ **9** → **11** →→ **15**) afforded intermediate **15** in ~5% overall yield from **5**, not taking the recycling step **16** → **14** into account.

**Structural Verification of the 2′-Amino-α-L-LNA Configuration.** In agreement with previously reported $^1$H NMR signals of other α-L-LNA nucleosides,[6b,9] the $^1$H NMR signals of H1′, H2′, and H3′ of 2′-amino-α-L-LNA nucleosides appear as singlets or narrow doublets ($J$ < 2 Hz)[20] since the H1′–C1′–C2′–H2′ and H2′–C2′–C3′–H3′ torsion angles are fixed in +*gauche* and −*gauche* conformations, respectively. The structure of bicyclic nucleoside **14** was ascertained by NOE difference spectroscopy. NOE contacts between H1′ and H2′ (7%), H1′ and H3′ (5%), and H2′ and H3′ (2%) suggested a *cis* relationship between these protons (Figure 2). Since the

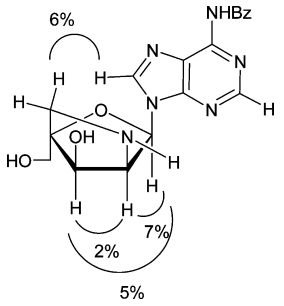


**Figure 2.** Key NOE contacts in nucleoside **14**.

stereochemical configuration at C3′ is defined by the choice of starting material and remains unchanged throughout synthesis, H1′ and H2′ must be pointing "down", which confirms the nucleobase as pointing "up" and hence establishes the 2′-amino-α-L-LNA configuration. This was substantiated by signal enhancements between $H5''_A$ and H8′ (6%), indicating a *cis* relationship between the nucleobase and H5″ ($H5''_A$ is tentatively assigned as the H5″ closest to the nucleobase).

**Synthesis of Phosphoramidite Building Blocks 1–4.** Chemoselective N2′-functionalizations of key intermediate **15** to give nucleosides **17**–**20** were realized as follows: (i) using 9′-fluorenylmethyl chloroformate to give **17** in 51% yield (Schotten–Baumann conditions could not be used because of the low solubility of **15** in dioxane/water); (ii) via reductive amination using 1-pyrenecarboxaldehyde and sodium triacetoxyborohydride[21] as the reducing agent to give **18** in 68% yield; or (iii) via EDC-mediated coupling of 1-pyrenecarboxylic acid or 1-pyreneacetic acid to give **19** in 64% yield and **20** in 79% yield, respectively (Scheme 4). Subsequent phosphitylation using 2-cyanoethyl-*N*,*N*′-diisopropylchlorophosphoramidite afforded the target compounds **1**–**4** in 46–71% yield after column chromatography and precipitation.

**Synthesis of Modified ONs and Experimental Design.** Phosphoramidites **1**–**4** were used in machine-assisted solid-phase DNA synthesis (0.2 μmol scale) to incorporate monomers **W**–**Z** into ONs using the following hand-coupling conditions (activator; coupling time; stepwise coupling yield): monomer **W** (pyridinium hydrochloride; 30 min; ~82%); monomers **X**–**Z** (pyridinium hydrochloride; 15 min; ~95%). Following workup and HPLC purification, the composition and purity of all of the modified ONs were ascertained by MALDI MS analysis (Tables S1 and S2 in the Supporting Information) and ion-pair reversed-phase HPLC, respectively. ONs containing a single incorporation in the 5′-GTG **B**TA TGC context are denoted **W1**, **X1**, **Y1**, and **Z1**, respectively. Similar conventions apply for ONs in the **B2**–**B6** series (see Table 1). Reference DNA and RNA strands are denoted as **D1**/**D2** and **R1**/**R2**, respectively. The following descriptive nomenclature is also


dx.doi.org/10.1021/jo4022937 | J. Org. Chem. 2013, 78, 12690–12702

**Scheme 4. Synthesis of Phosphoramidites 1−4**[a]

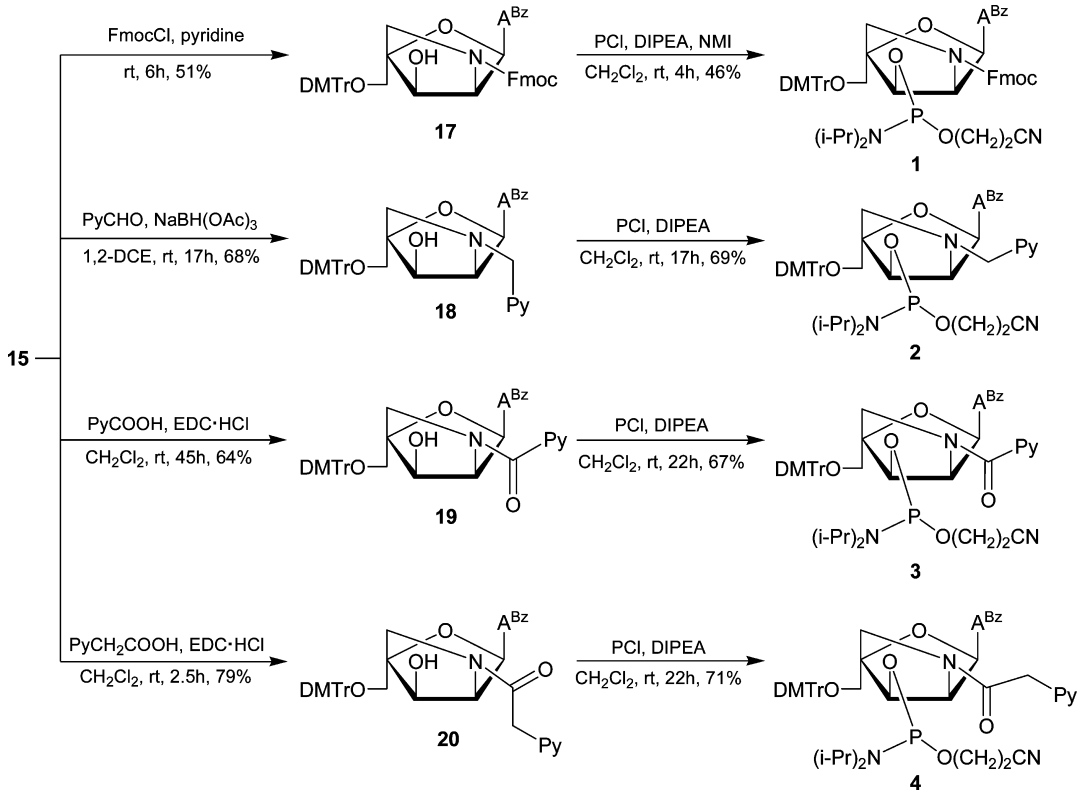


[a]Abbreviations: $A^{Bz}$ = 6-*N*-benzoyladenin-9-yl; DIPEA = *N*,*N*′-diisopropylethylamine; DMTr = 4,4′-dimethoxytrityl; EDC·HCl = 1-ethyl-3-(3-dimethylaminopropyl)carbodiimide hydrochloride; FmocCl = 9′-fluorenylmethyl chloroformate; NMI = *N*-methylimadazole; PCl = 2-cyanoethyl-*N*,*N*′-diisopropylchlorophosphoramidite; Py = pyren-1-yl.

used: N2′-PyMe (**X** series), N2′-PyCO (**Y** series) and N2′-PyAc (**Z** series). We previously used this 9-mer mixed-sequence context to study the hybridization properties of ONs modified with N2′-pyrene-functionalized 2′-amino-α-L-LNA-thymine monomers, which facilitates a direct comparison.[9]

**Thermal Denaturation Experiments.** *Thermal Affinity toward Complementary DNA/RNA.* The thermostabilities of duplexes between **W**/**X**/**Y**/**Z**-modified ONs and complementary DNA/RNA were evaluated by determining their thermal denaturation temperatures ($T_m$) in medium-salt buffer ([$Na^+$] = 110 mM, pH 7.0). The changes in $T_m$ for the modified duplexes relative to the $T_m$ values for the unmodified reference duplexes ($\Delta T_m$) are discussed.

ONs with one or two incorporations of 2′-amino-α-L-LNA-adenine monomer **W** display very similar thermal affinities toward complementary DNA as the unmodified reference ONs ($\Delta T_m$ between −1.0 to +0.5 °C; Table 1). Thus, unlike the corresponding 2′-oxy-α-L-LNA-adenine monomer,[6b,22] the 2-oxo-5-azabicyclo[2.2.1]heptane skeleton of monomer **W** is not inherently beneficial for DNA duplex formation. We have made similar observations with ONs modified with the thymine counterpart of monomer **W**.[9a] This indicates that the unfunctionalized 2′-nitrogen of 2′-amino-α-L-LNA monomers either stabilizes the single-stranded ON or destabilizes the duplex, for example, by perturbing the hydration spine in the major groove. In contrast, ONs modified with N2′-pyrene-functionalized 2′-amino-α-L-LNA-adenine monomer **X**, **Y**, or **Z** display greatly increased thermal affinity toward DNA targets ($\Delta T_m$/modification between +2.5 and +14 °C; Table 1). The observed $T_m$ trends for singly modified ONs (**Y** > **Z** ≥ **X**) indicate that (i) monomers in which the pyrene moiety is attached to the 2-oxo-5-azabicyclo[2.2.1]heptane skeleton via an alkanoyl linker induce greater thermostabilization than the corresponding monomers employing alkyl linkers (N2′-PyCO

**Table 1. $\Delta T_m$ Values for Duplexes between B1−B6 and Complementary DNA Targets**[a]

| ON | duplex | $\Delta T_m$/°C B = W | B = X | B = Y | B = Z |
|---|---|---|---|---|---|
| **B1**<br>**D2** | 5′-GTG **B**TA TGC<br>3′-CAC TAT ACG | −0.5 | +5.0 | +11.0 | +6.0 |
| **B2**<br>**D2** | 5′-GTG AT**B** TGC<br>3′-CAC TAT ACG | +0.5 | +7.0 | +14.0 | +7.5 |
| **B3**<br>**D2** | 5′-GTG **B**T**B** TGC<br>3′-CAC TAT ACG | −1.0 | +5.0 | +13.5 | +16.0 |
| **D1**<br>**B4** | 5′-GTG ATA TGC<br>3′-CAC T**B**T ACG | ±0.0 | +6.5 | +11.5 | +7.5 |
| **D1**<br>**B5** | 5′-GTG ATA TGC<br>3′-CAC TAT **B**CG | ±0.0 | +5.5 | +12.0 | +6.0 |
| **D1**<br>**B6** | 5′-GTG ATA TGC<br>3′-CAC T**B**T **B**CG | −2.0 | +5.0 | +13.5 | +14.5 |

[a]$\Delta T_m$ = change in $T_m$ relative to the value for the unmodified reference duplex **D1**:**D2** ($T_m \equiv 27.5$ °C). $T_m$ was determined as the maximum of the first derivative of the melting curve ($A_{260}$ vs $T$) recorded in medium-salt buffer ([$Na^+$] = 110 mM, [$Cl^-$] = 100 mM, pH 7.0 ($NaH_2PO_4/Na_2HPO_4$)) using a concentration of 1.0 μM for each strand. $T_m$ values are averages of at least two measurements within 1.0 °C. A/C/G/T = adenin-9-yl/cytosin-1-yl/guanin-9-yl/thymin-1-yl DNA monomers. For the structures of monomers **W**−**Z**, see Figure 1. Data for the **B1**, **B2**, **B4**, and **B5** series for monomers **X**, **Y**, and **Z** were previously reported in ref 12b.


dx.doi.org/10.1021/jo4022937 | J. Org. Chem. 2013, 78, 12690−12702

**Y** > N2′-PyMe **X**) and (ii) monomers with short alkanoyl linkers result in more thermostable DNA duplexes than the corresponding monomers with longer alkanoyl linkers (N2′-PyCO **Y** > N2′-PyAc **Z**). We previously observed similar structure−property relationships with the analogous thymine monomers, which on the basis of UV−vis spectroscopy and molecular modeling results were explained by differential placement of the pyrene moiety for affinity-enhancing intercalation.[9b] Similar structural underpinnings are likely in effect for monomers **X**−**Z** (vide infra). However, the electron density of the pyrene moieties, which differs among the three monomers, may also be a contributing factor to the differential duplex stabilization.

An interesting trend was observed for the doubly modified ONs: incorporation of a second N2′-PyMe **X** or N2′-PyCO **Y** monomer did not result in additionally increased thermal affinity against DNA targets, whereas a second incorporation of the more flexible N2′-PyAc **Z** monomer did (compare the $\Delta T_m$ values for the **B1**−**B3** and **B4**−**B6** series in Table 1). We hypothesize that the former observation is due to violation of the "nearest-neighbor exclusion principle", which states that free intercalators at most bind to every second base pair of a DNA duplex because of limits on the local expandability of duplexes.[23] If the principle is extrapolated to tethered intercalators and 3′-intercalative binding modes of the pyrene moieties of monomers **X**−**Z** are assumed (vide infra), the resulting duplexes involving **B3** and **B6** would feature a localized region with two intercalators in an area defined by four base pairs, which is at the saturation threshold. We speculate that the greater flexibility of the N2′-PyAc **Z** monomer allows the modified DNA duplexes to structurally compensate for any stress induced by the high intercalator density.

Interestingly, the modified ONs displayed rather different thermal denaturation characteristics with RNA targets. ONs modified with 2′-amino-$\alpha$-L-LNA adenine monomer **W** displayed significantly higher affinity against RNA than DNA targets ($\Delta T_m$/modification between +1.5 and +7.0 °C; Table 2). Further, **X**- and **Y**-modified ONs displayed markedly lower thermal affinities toward RNA than DNA targets, with N2′-PyMe **X**-modified DNA:RNA duplexes displaying similar thermostabilities as unmodified reference duplexes ($\Delta T_m$/modification between −0.5 and +2.5 °C; Table 2) and N2′-PyCO **Y**-modified duplexes being moderately stabilized ($\Delta T_m$/modification between +1.5 and +6.5 °C; Table 2). N2′-PyAc **Z**-modified ONs also displayed lower affinities toward RNA than DNA targets but resulted in more thermostable heteroduplexes ($\Delta T_m$/modification between +4.0 and +8.0 °C; Table 2). These differences may again reflect the greater flexibility of monomer **Z**, which allows the pyrene moieties to adopt more favorable positions for affinity-enhancing intercalation (vide infra). DNA-selective hybridization (Table S3 in the Supporting Information), as seen for **X**/**Y**/**Z**-modified ONs and ONs modified with the thymine counterparts,[9b] is often observed for ONs modified with intercalating moieties,[24] as intercalators favor the B-type helix geometry of DNA:DNA duplexes over the more compressed A/B-type helix geometry of DNA:RNA duplexes.[25]

**Table 2. $\Delta T_m$ Values for Duplexes between B1−B6 and Complementary RNA Targets[a]**

| | | $\Delta T_m$/°C | | | |
|---|---|---|---|---|---|
| ON | duplex | **B** = **W** | **B** = **X** | **B** = **Y** | **B** = **Z** |
| **B1**<br>**R2** | 5′-GTG **B**TA TGC<br>3′-CAC UAU ACG | +2.5 | −1.0 | +1.5 | +4.0 |
| **B2**<br>**R2** | 5′-GTG AT**B** TGC<br>3′-CAC UAU ACG | +2.5 | +1.0 | +5.0 | +4.5 |
| **B3**<br>**R2** | 5′-GTG **B**T**B** TGC<br>3′-CAC UAU ACG | +3.0 | −1.5 | +4.5 | +11.0 |
| **R1**<br>**B4** | 5′-GUG AUA UGC<br>3′-CAC T**B**T ACG | +4.5 | −0.5 | +2.5 | +6.5 |
| **R1**<br>**B5** | 5′-GUG AUA UGC<br>3′-CAC TAT **B**CG | +7.0 | +2.5 | +6.5 | +8.0 |
| **R1**<br>**B6** | 5′-GUG AUA UGC<br>3′-CAC T**B**T **B**CG | +7.0 | ±0.0 | +7.0 | +14.5 |

[a]$\Delta T_m$ = change in $T_m$ relative to the value for the unmodified reference duplex **D1**:**R2** ($T_m \equiv$ 26.0 °C) or **R1**:**D2** ($T_m \equiv$ 24.5 °C); for conditions of the thermal denaturation experiments, see Table 1.

*Mismatch Discrimination.* The binding specificities of centrally modified ONs against DNA/RNA strands with mismatched nucleotides opposite the **W**−**Z** monomers were determined. **W4** displayed improved discrimination of mismatched DNA targets relative to reference strand **D2**, with the AG mismatch being discriminated particularly well (Table 3).

**Table 3. Discrimination of Mismatched DNA Targets by B4 Series and Reference ONs[a]**

| | | DNA: 5′-GTG A**B**A TGC | | | |
|---|---|---|---|---|---|
| | | $T_m$/°C | $\Delta T_m$/°C | | |
| ON | sequence | **B** = T | **B** = A | **B** = C | **B** = G |
| **D2** | 3′-CAC TAT ACG | **27.5** | −17.0 | −15.5 | −9.0 |
| **W4** | 3′-CAC T**W**T ACG | **27.5** | −20.0 | −17.0 | −16.0 |
| **X4** | 3′-CAC T**X**T ACG | **34.0** | −16.5 | −7.5 | −17.0 |
| **Y4** | 3′-CAC T**Y**T ACG | **39.0** | −21.0 | −12.0 | −17.0 |
| **Z4** | 3′-CAC T**Z**T ACG | **35.0** | −21.5 | −14.0 | −14.5 |

[a]For conditions of the thermal denaturation experiments, see Table 1. $T_m$ values for the fully matched duplexes are shown in bold. $\Delta T_m$ = change in $T_m$ relative to the value for the fully matched DNA:DNA duplex.

**X4**/**Y4**/**Z4** displayed surprisingly efficient discrimination of mismatched DNA targets, particularly of AG mismatches (Table 3), considering the likely intercalative binding mode of the pyrene moieties, which is known to typically decrease base-pairing fidelity.[9b,26] However, ONs with **X**/**Y**/**Z** monomers positioned as next-nearest neighbors displayed poor discrimination of the centrally mismatched DNA target (**B3** series; Table S4 in the Supporting Information), indicating that the modification pattern has a major influence on the binding specificity. Discrimination of RNA mismatches was generally less efficient with **W4**/**X4**/**Y4** than with reference ONs but improved with **Z4** (Table 4).

**Optical Spectroscopy.** UV−vis absorption and steady-state fluorescence emission spectra of **X**/**Y**/**Z**-modified ONs and the corresponding duplexes with DNA/RNA targets were recorded to gain additional insight into the binding modes of the pyrene moieties of monomers **X**/**Y**/**Z**. Bathochromic shifts of pyrene absorption maxima, which are indicative of strong interactions between pyrenes and nucleobases,[27] were generally observed upon hybridization with complementary DNA/RNA ($\Delta\lambda_{max}$ = 0−6 nm; Table 5, Figure 3, and Figures S2 and S3 in the Supporting Information), with the most pronounced increases being observed for duplex formation of **Y**-modified ONs with DNA. These results are consistent with intercalative binding modes for the pyrene moieties of monomers **X**/**Y**/**Z**


dx.doi.org/10.1021/jo4022937 | J. Org. Chem. 2013, 78, 12690−12702

**Table 4. Discrimination of Mismatched RNA Targets by B4 Series and Reference ONs[a]**

| | | RNA: 5′-GUG A**B**A UGC | | | |
|---|---|---|---|---|---|
| | | $T_m$/°C | $\Delta T_m$/°C | | |
| ON | sequence | **B** = U | **B** = A | **B** = C | **B** = G |
| **D2** | 3′-CAC TAT ACG | **24.5** | −15.0 | −15.0 | −11.0 |
| **W4** | 3′-CAC T**W**T ACG | **29.0** | −13.5 | −13.0 | −11.5 |
| **X4** | 3′-CAC T**X**T ACG | **24.0** | −10.5 | −8.0 | −10.0 |
| **Y4** | 3′-CAC T**Y**T ACG | **27.0** | −10.5 | −11.0 | −8.5 |
| **Z4** | 3′-CAC T**Z**T ACG | **31.0** | −19.0 | −15.5 | −14.5 |

[a]For conditions of the thermal denaturation experiments, see Table 1. $T_m$ values for the fully matched duplexes are shown in bold. $\Delta T_m$ = change in $T_m$ relative to the value for the fully matched RNA:DNA duplex.

and in agreement with our previous observations for the corresponding thymine analogues.[9b]

Steady-state fluorescence emission spectra were recorded at 5 °C using an excitation wavelength of $\lambda_{ex}$ = 350 nm. Hybridization of N2′-PyMe **X**-modified or N2′-PyAc **Z**-modified ONs with complementary DNA/RNA resulted in decreased emission (Figure 3 and Figures S4 and S7 in the Supporting Information), which is consistent with intercalation-induced quenching by flanking nucleobases.[27,28] The resulting duplexes were only weakly fluorescent and exhibited defined vibronic bands at ∼380 nm and ∼400 nm along with a shoulder at 420−425 nm. On the other hand, a range of responses was observed upon hybridization of N2′-PyCO **Y**-modified ONs with complementary DNA/RNA, varying from ∼50% reduction to ∼3-fold enhancement of emission (Figure S5 in the Supporting Information). The resulting duplexes were strongly fluorescent (nearly 2 orders of magnitude more fluorescent than **X**-modified duplexes) with little or no vibronic fine structure ($\lambda_{em,max} \approx$ 400 nm, broad band). The lack of a consistent response upon hybridization to DNA/RNA presumably is not due to different pyrene binding modes in the resulting duplexes but rather reflects different fluorescence intensities of the single-stranded probes, possibly due to different sequence-dependent rotational barriers around the Py−CO bond. Thus, singly modified DNA duplexes displayed similar emission intensities (Figure S6 in the Supporting Information), suggesting that the pyrene moieties are in similar microenvironments in the duplex, which is consistent with an intercalative binding mode.

To further substantiate the proposed intercalative binding mode of N2′-PyCO monomer **Y**, we synthesized three additional **Y**-modified ONs in which the 3′-flanking nucleotide was varied systematically (**Y7**−**Y9**, Table 6). ONs with 3′-flanking purines displayed greater relative increases in thermal affinity against DNA targets than the corresponding ONs with 3′-flanking pyrimidines (compare the $\Delta T_m$ values for **Y7**:**D3** and **Y9**:**D5** with those for **Y8**:**D4** and **Y4**:**D1** in Table 6). This is consistent with the proposed binding mode, as 3′-intercalating pyrenes are expected to interact more strongly with large purines.

Steady-state fluorescence emission experiments provided further evidence for an intercalative binding mode of the pyrenes, as the emission levels of these four DNA duplexes decreased in the anticipated order of nucleobase quenching efficiency (from least to most quenched: 3′-flanking A > T > C > G; Figure 4).[28b,29]

## CONCLUSION

ONs modified with N2′-pyrene-functionalized 2′-amino-α-L-LNA-adenine monomers **X**−**Z** display very high affinity toward DNA targets. The DNA-selective hybridization, together with hybridization-induced bathochromic shifts of pyrene absorption maxima and quenching of pyrene fluorescence, is indicative of intercalative binding modes for the pyrene moieties. ONs with such characteristics are likely to be of significant interest for applications in nucleic acid diagnostics and biotechnology.[30] However, the synthesis of the corresponding phosphoramidites is very challenging because of nontrivial protecting-group manipulations (<1% overall yield from diacetone-α-D-glucose), which emphasizes the need for a more efficient synthetic route toward these building blocks or access to functional analogues of N2′-functionalized 2′-amino-α-L-LNA monomers, which are easier to synthesize. In fact, we have already discovered the first examples of such analogues, namely, N2′-pyrene-functionalized 2′-*N*-methyl-2′-amino-DNA and O2′-pyrene-functionalized RNA monomers,[8a,12b] and are exploring their use for applications in nucleic acid diagnostics.[8b,c]

## EXPERIMENTAL SECTION

**9-[2-*O*-Acetyl-3-*O*-benzyl-5-*O*-methanesulfonyl-4-*C*-methanesulfonyloxymethyl-α-L-*threo*-pentofuranosyl]-6-*N*-benzoyladenine (6).** 6-*N*-Benzoyladenine (28.6 g, 0.12 mol) and glycosyl donor **5**[6b] (40.6 g, 79.8 mmol) were coevaporated with 1,2-dichloroethane (2 × 150 mL) and resuspended in anhydrous 1,2-dichloroethane (270 mL). To this was added *N*,*O*-bis(trimethylsilyl)-

**Table 5. Absorption Maxima in the 300−400 nm Region for ONs Modified with N2′-Pyrene-Functionalized 2′-Amino-α-L-LNA Adenine Monomers X/Y/Z in the Presence or Absence of Complementary DNA/RNA Targets[a]**

| | | $\lambda_{max}$/nm [$\Delta\lambda_{max}$/nm] | | | | | | | | |
|---|---|---|---|---|---|---|---|---|---|---|
| | | **B** = X | | | **B** = Y | | | **B** = Z | | |
| ON | sequence | SSP | +DNA | +RNA | SSP | +DNA | +RNA | SSP | +DNA | +RNA |
| **B1** | 5′-GTG **B**TA TGC | 348 | 350 [+2] | 350 [+2] | 349 | 352 [+3] | 351 [+2] | 348 | 350 [+2] | 351 [+3] |
| **B2** | 5′-GTG ATB TGC | 348 | 350 [+2] | 349 [+1] | 349 | 353 [+4] | 351 [+2] | 350 | 351 [+1] | 351 [+1] |
| **B3** | 5′-GTG **B**T**B** TGC | 347 | 349 [+2] | 348 [+1] | 349 | 351 [+2] | 351 [+2] | 347 | 350 [+3] | 351 [+4] |
| **B4** | 3′-CAC T**B**T ACG | 348 | 350 [+2] | 348 [±0] | 347 | 353 [+6] | 352 [+5] | 348 | 351 [+3] | 351 [+3] |
| **B5** | 3′-CAC TAT **B**CG | 348 | 350 [+2] | 350 [+2] | 350 | 351 [+1] | 350 [±0] | 348 | 351 [+3] | 351 [+3] |
| **B6** | 3′-CAC T**B**T **B**CG | 348 | 350 [+2] | 348 [±0] | 348 | 352 [+4] | 353 [+5] | 348 | 351 [+3] | 351 [+3] |

[a]$\Delta\lambda_{max}$ = change in absorption maximum relative to $\lambda_{max}$ for the single-stranded probe (SSP). Measurements were performed at 5 °C except for the single-stranded **X**/**Y**-modified probes, whose spectra were recorded at room temperature. Buffer conditions were the same as in the thermal denaturation experiments.


dx.doi.org/10.1021/jo4022937 | J. Org. Chem. 2013, 78, 12690−12702

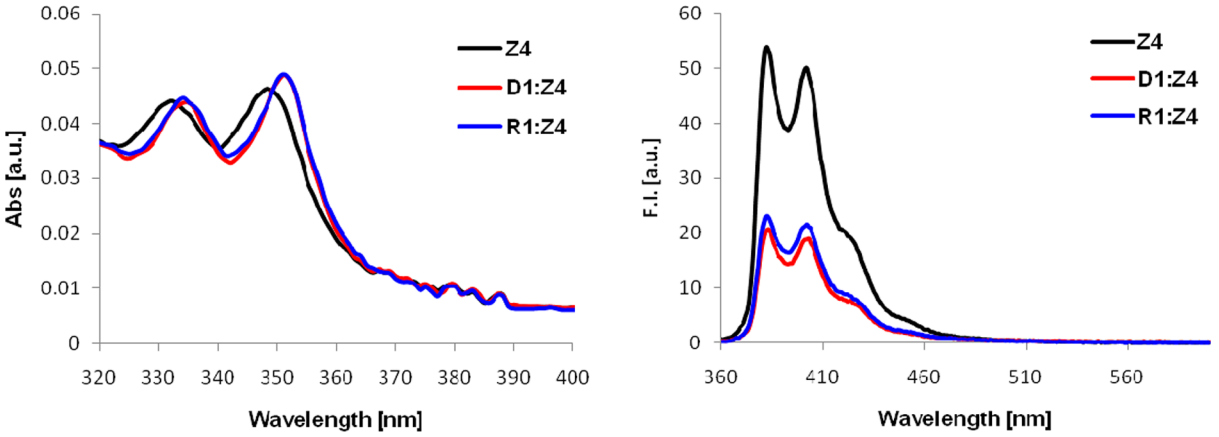


**Figure 3.** (left) UV−vis absorption and (right) steady-state fluorescence emission spectra of **Z4** in the presence or absence of complementary DNA/RNA. $T_{exp}$ = 5 °C; each ON was used at 1 $\mu$M concentration in $T_m$ buffer; $\lambda_{ex}$ = 350 nm (fluorescence).

**Table 6. $T_m$ Values for Duplexes between Y4/Y7/Y8/Y9 and Complementary DNA Targets[a]**

| ON | duplex | $\Delta T_m$/°C | reference $T_m$/°C |
|---|---|---|---|
| **D3**<br>**Y7** | 5′-GTG TT ATGC<br>3′-CAC A**Y** TACG | +17.0 | 27.5 |
| **D4**<br>**Y8** | 5′-GTG GT ATGC<br>3′-CAC C**Y** TACG | +10.0 | 33.0 |
| **D5**<br>**Y9** | 5′-GTG CT ATGC<br>3′-CAC G**Y** TACG | +19.5 | 24.0[b] |
| **D1**<br>**Y4** | 5′-GTG AT ATGC<br>3′-CAC T**Y** TACG | +11.5 | 27.5 |

[a]$\Delta T_m$ = change in $T_m$ relative to the value for the unmodified reference duplex. For experimental conditions, see Table 1. [b]The low $T_m$ of this reference duplex was confirmed by two independent operators using strands from three different commercial batches.

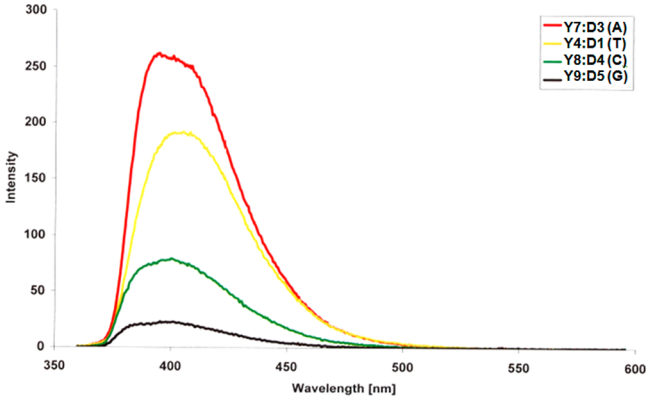


**Figure 4.** Fluorescence emission spectra of duplexes between **Y4**/**Y7**/**Y8**/**Y9** and complementary DNA targets. The nucleotide flanking the **Y** monomer on its 3′-side is listed in the parentheses. $T_{exp}$ = 5 °C; each ON used at 0.15 $\mu$M concentration in $T_m$ buffer; $\lambda_{ex}$ = 350 nm.

acetamide (BSA) (49.2 mL, 0.20 mol), and the suspension was heated at reflux until it turned homogeneous. The solution was then cooled to rt. TMSOTf (43.1 mL, 0.24 mol) was slowly added, and the reaction mixture was heated at reflux for 70 h. The mixture was then cooled to rt and slowly poured into a solution of sat. aq. $NaHCO_3$ and crushed ice (500 mL, 1:1 v/v). Additional crushed ice (~400 mL) was added, and the mixture was stirred for 30 min. The resulting precipitate was removed via filtration, and the filtrate was extracted with $CH_2Cl_2$ (1.5 L). The organic layer was washed with sat. aq. $NaHCO_3$ (2 × 500 mL), and the combined aqueous layer was back-extracted with $CH_2Cl_2$ (2 × 500 mL). The combined organic layer was evaporated to afford a crude residue, which was purified by silica gel column chromatography (0−10% v/v *i*-PrOH in $CH_2Cl_2$) to provide nucleoside **6** (38.3 g, 70%) as a white foam. $R_f$ = 0.4 (5% v/v MeOH in $CH_2Cl_2$); MALDI-HRMS *m*/*z* 712.1380 ($[M + Na]^+$, $C_{29}H_{31}N_5O_{11}S_2{\cdot}Na^+$, calcd 712.1354). The observed $^{13}C$ NMR data (75.5 MHz, $CDCl_3$) are in good agreement with previously reported data for this compound.[6b]

**9-[3-*O*-Benzyl-5-*O*-methanesulfonyl-4-*C*-methanesulfonyloxymethyl-α-L-*threo*-pentofuranosyl]-6-*N*-benzoyladenine (7).** Fully protected nucleoside **6** (4.66 g, 6.76 mmol) was dissolved in a solution[17] of guanidinium nitrate (4.91 g, 40.2 mmol) and NaOMe (0.24 g, 4.44 mmol) in MeOH:$CH_2Cl_2$ (450 mL, 9:1 v/v). The reaction mixture was stirred at rt for 30 min, at which point sat. aq. $NH_4Cl$ (200 mL) was added. The resulting white precipitate was filtered off and washed with $CH_2Cl_2$, and the filtrate was concentrated. The aqueous layer was extracted with $CH_2Cl_2$ (5 × 200 mL), and the combined organic layers were evaporated to near dryness. The resulting crude residue was purified by silica gel column chromatography (0−4% v/v MeOH in $CH_2Cl_2$) to afford alcohol **7** (3.84 g, 88%) as a white foam. $R_f$ = 0.5 (10% v/v MeOH in $CH_2Cl_2$); MALDI-HRMS *m*/*z* 670.1234 ($[M + Na]^+$, $C_{27}H_{29}N_5O_{10}S_2{\cdot}Na^+$, calcd 670.1248). The observed $^{13}C$ NMR data (75.5 MHz, $CDCl_3$) are in good agreement with previously reported data for this compound.[6b]

**9-[2-*C*-Azido-3-*O*-benzyl-2-deoxy-4-*C*-methanesulfonyloxymethyl-5-*O*-methanesulfonyl-α-L-*erythro*-pentofuranosyl]-6-*N*-benzoyladenine (8).** Alcohol **7** (18.6 g, 28.7 mmol) was coevaporated with anhydrous pyridine (50 mL) and dissolved in anhydrous $CH_2Cl_2$ (200 mL). The solution was cooled to −78 °C, and anhydrous pyridine (7.3 mL, 90.6 mmol) was added, followed by dropwise addition of trifluoromethanesulfonyl anhydride ($Tf_2O$) (9.90 mL, 58.9 mmol). The reaction mixture was allowed to warm to rt and stirred for 3 h. At this point, crushed ice (50 mL) was added, and the layers were separated. The organic layer was washed with sat. aq. $NaHCO_3$ (2 × 50 mL), evaporated to near dryness, and coevaporated with abs. EtOH (2 × 50 mL) to afford the crude O2′-triflate as a light-brown residue, which was used in the next step without further purification.

$NaN_3$ (19.6 g, 0.30 mol) and 15-crown-5 (6.0 mL, 0.30 mol) were added to a solution of the crude O2′-triflate in anhydrous DMF (300 mL). The reaction mixture was stirred first at rt for 15 h and then for an additional 8 h at 50 °C. After the mixture was cooled to rt, the solids were filtered off and washed with EtOAc, and the combined organic layers were concentrated until near dryness. The concentrate was taken up in EtOAc (200 mL) and brine (200 mL), and the layers were separated, after which the aqueous layer extracted with EtOAc (4 × 100 mL). The combined organic layers were evaporated to near dryness, and the resulting crude residue was purified by silica gel column chromatography (0−90% v/v EtOAc in petroleum ether) to afford azide **8** (17.9 g, 89% over two steps) as a white solid material. $R_f$ = 0.4 (EtOAc); IR (KBr) 2116 $cm^{-1}$ ($N_3$); MALDI-HRMS *m*/*z* 695.1295 ($[M + Na]^+$, $C_{27}H_{28}N_8O_9S_2{\cdot}Na^+$, calcd 695.1313); $^1H$ NMR


dx.doi.org/10.1021/jo4022937 | J. Org. Chem. 2013, 78, 12690−12702

(300 MHz, DMSO-$d_6$) $\delta$ 11.30 (s, 1H, ex), 8.79 (s, 1H), 8.54 (s, 1H), 8.05 (d, 2H, $J$ = 7.0 Hz), 7.30−7.67 (m, 8H), 6.74 (d, 1H, $J$ = 4.4 Hz), 5.08−5.16 (m, 1H), 4.89 (d, 1H, $J$ = 5.1 Hz), 4.74−4.83 (m, 2H), 4.69−4.72 (d, 1H, $J$ = 11.4 Hz), 4.47−4.51 (d, 1H, $J$ = 11.4 Hz), 4.42 (s, 2H), 3.28 (s, 3H), 3.24 (s, 3H); $^{13}$C NMR (75.5 MHz, DMSO-$d_6$) $\delta$ 151.9, 150.4, 142.7, 136.9, 133.2, 132.5, 128.5, 128.0, 81.9, 81.7, 80.1, 73.5, 68.3, 61.9, 36.98, 36.94. The carbonyl group of the 6-*N*-benzoyl group was not visible.

**(1*S*,3*R*,4*S*,7*R*)-3-(6-*N*-Benzoyladenin-9-yl)-7-benzyloxy-1-methanesulfonyloxymethyl-2-oxa-5-azabicyclo[2.2.1]heptane (9).** Aqueous NaOH (2 M, 38.9 mL, 77.8 mmol) and trimethylphosphine (1 M in THF, 77.8 mL, 77.8 mmol) were added to an ice-cold solution of azido nucleoside **8** (35.2 g, 51.8 mmol) in THF (500 mL). The reaction mixture was allowed to warm to rt and was stirred at this temperature for 21 h. The mixture was then evaporated to near dryness, and the resulting crude residue taken up in EtOAc (200 mL) and brine (200 mL). After the layers were separated, the aqueous layer was extracted with MeOH:$CH_2Cl_2$ (3 × 200 mL, 2:8 v/v). The combined organic layers were evaporated to dryness, and the resulting crude material was purified by silica gel column chromatography (0−5% v/v MeOH in $CH_2Cl_2$) to provide bicyclic nucleoside **9** (24.2 g, 85%) as a solid brown material. $R_f$ = 0.3 (EtOAc); MALDI-HRMS $m/z$ 573.1517 ([M + Na]$^+$, $C_{26}H_{26}N_6O_6S{\cdot}Na^+$, calcd 573.1527); $^1$H NMR[31] (500 MHz, DMSO-$d_6$) $\delta$ 11.17 (s, 1H, ex, NH), 8.77 (s, 1H, H8), 8.73 (s, 1H, H2), 8.06 (d, 2H, $J$ = 7.0 Hz, Bz), 7.54−7.67 (m, 3H, Bz), 7.29−7.47 (m, 5H, Ph), 6.52 (d, 1H, $J$ = 1.8 Hz, H1′), 4.72−4.76 (d, 1H, $J$ = 11.7 Hz, $CH_2$Ph), 4.62−4.67 (d, 1H, $J$ = 11.7 Hz, $CH_2$Ph), 4.57−4.60 (d, 1H, $J$ = 11.7 Hz, H5′$_A$), 4.49−4.53 (d, 1H, $J$ = 11.7 Hz, H5′$_B$), 4.45 (s, 1H, H3′), 3.93 (br s, 1H, H2′), 3.28−3.31 (m, 1H, H5″$_A$, partial overlap with $H_2O$), 3.22 (s, 3H, $CH_3SO_2$), 3.10−3.13 (d, 1H, $J$ = 9.9 Hz, H5″$_B$); $^{13}$C NMR (125 MHz, DMSO-$d_6$) $\delta$ 165.5, 152.1, 151.4 (C2), 150.0, 143.1 (C8), 137.8, 133.3, 132.3 (Bz), 128.4 (Ar), 128.2 (Ar), 127.62 (Ar), 127.60 (Ar), 125.1, 87.2, 84.3 (C1′), 80.4 (C3′), 71.0 ($CH_2$Ph), 66.8 (C5′), 59.8 (C2′), 51.1 (C5″), 36.8 ($CH_3SO_2$). The $^1$H and $^{13}$C NMR data are in reasonable agreement with previously reported data from the patent literature.[18] The 2-oxo-5-azabicyclo[2.2.1]heptane skeleton and stereochemistry of **9** were verified via NOE experiments on downstream product **14**.

**(1*S*,3*R*,4*S*,7*R*)-3-(6-*N*-Benzoyladenin-9-yl)-7-benzyloxy-1-methanesulfonyloxymethyl-5-trifluoroacetyl-2-oxa-5-azabicyclo[2.2.1]heptane (11).** Bicyclic nucleoside **9** (8.68 g, 15.8 mmol) was coevaporated with pyridine (2 × 20 mL) and dissolved in anhydrous $CH_2Cl_2$ (200 mL) and anhydrous pyridine (5.09 mL, 63 mmol). The solution was cooled to 0 °C, and trifluoroacetic acid anhydride (4.45 mL, 31.5 mmol) was added. The reaction mixture was stirred for 2 h at 0 °C, at which point crushed ice (50 mL) was added. The layers were separated, and the organic layer was washed with sat. aq. $NaHCO_3$ (2 × 50 mL). The combined aqueous layers were back-extracted with $CH_2Cl_2$ (2 × 100 mL) and MeOH:$CH_2Cl_2$ (100 mL, 2:8 v/v), and the combined organic layers were evaporated to near dryness. The resulting crude residue was sequentially coevaporated with toluene (50 mL) and abs. EtOH:toluene (50 mL, 1:1 v/v) and purified by silica gel column chromatography (0−100% v/v EtOAc in petroleum ether) to afford fully protected nucleoside **11** (6.27 g, 62%) as a white foam. $R_f$ = 0.5 (10% v/v MeOH:EtOAc). Physical data for the mixture of rotamers (~4:6 by $^1$H NMR): MALDI-HRMS $m/z$ 647.1541 ([M + H]$^+$, $C_{28}H_{25}F_3N_6O_7S{\cdot}H^+$, calcd 647.1530); $^1$H NMR[31,32] (500 MHz, DMSO-$d_6$) $\delta$ 11.21 (s, 0.6H, ex, NH$_B$), 11.19 (s, 0.4H, ex, NH$_A$), 8.78 (s, 0.6H, H2$_B$), 8.76 (s, 0.4H, H2$_A$), 8.63 (s, 0.4H, H8$_A$), 8.60 (s, 0.6H, H8$_B$), 8.05 (d, 2H, $J$ = 7.0 Hz, Bz$_{A+B}$), 7.52−7.67 (m, 3H, Bz$_{A+B}$), 7.31−7.41 (m, 5H, Ph$_{A/B}$), 6.83 (d, 0.6H, $J$ = 1.1 Hz, H1′$_B$), 6.80 (d, 0.4H, $J$ = 1.1 Hz, H1′$_A$), 5.26 (s, 0.4H, H2′$_A$), 5.17 (s, 0.6H, H2′$_B$), 4.84 (s, 0.6H, H3′$_B$), 4.82 (s, 0.4H, H3′$_A$), 4.62−4.79 (m, 4H, $CH_2$Ph$_{A+B}$, H5′$_{A+B}$), 4.53 (d, 0.4H, $J$ = 10.6 Hz, H5″$_A$), 4.35 (d, 0.6H, $J$ = 12.1 Hz, H5″$_B$), 4.07 (d, 0.4H, $J$ = 10.6 Hz, H5″$_A$), 3.91 (d, 0.6H, $J$ = 12.1 Hz, H5″$_B$), 3.28 (s, 3H, $CH_3SO_2$); $^{13}$C NMR (125 MHz, DMSO-$d_6$) $\delta$ 165.49, 165.48, 155.3 (q, $J$ = 37 Hz, $COCF_3$), 155.0 (q, $J$ = 37 Hz, $COCF_3$), 151.8 (C2$_B$), 151.65 (C2$_A$), 151.59, 150.4, 150.3, 141.2 (C8$_B$), 141.0 (C8$_A$), 137.2, 137.0, 133.3, 132.4 (Bz), 128.43 (Bz), 128.40 (Ar), 128.39 (Ar), 128.38 (Ar), 128.34 (Ph), 127.91 (Ph), 127.88 (Ph), 127.53 (Ph), 127.51 (Ph), 125.5, 125.3, 115.5 (q, $J$ = 288 Hz, $CF_3$), 115.2 (q, $J$ = 288 Hz, $CF_3$), 86.16, 86.15, 84.9 (C1′$_A$), 84.0 (C1′$_B$), 79.2 (C3′$_B$), 77.4 (C3′$_A$), 71.6 ($CH_2$Ph), 65.3 (C5′), 65.0 (C5′), 63.0 (C2′$_B$), 61.4 (C2′$_A$), 53.2 (C5″$_B$), 53.1 (C5″$_A$), 37.0 ($CH_3SO_2$); $^{19}$F NMR (376 MHz, DMSO-$d_6$) $\delta$ −71.3 ($CF_{3,B}$), −72.1 ($CF_{3,A}$).

**(1*S*,3*R*,4*S*,7*R*)-3-(6-*N*-Benzoyladenin-9-yl)-7-hydroxy-1-methanesulfonyloxymethyl-5-trifluoroacetyl-2-oxa-5-azabicyclo[2.2.1]heptane (12).** Fully protected nucleoside **11** (19.6 g, 30.4 mmol) was coevaporated with 1,2-dichloroethane (3 × 100 mL) and dissolved in anhydrous $CH_2Cl_2$ (600 mL). The solution was cooled to −78 °C, and $BCl_3$ (1 M solution in hexanes, 370 mL, 0.37 mol) was added. The reaction mixture was allowed to warm to rt and was stirred for 17 h. The mixture was then cooled to 0 °C, and crushed ice (800 mL) was slowly added. The layers were separated, and the organic phase was washed with sat. aq. $NaHCO_3$ (2 × 300 mL). The combined aqueous layers were back-extracted with EtOAc (4 × 500 mL), and the combined organic phases were evaporated to near dryness. The resulting residue was purified using silica gel column chromatography (0−20% v/v MeOH in $CH_2Cl_2$) to afford alcohol **12** (14.7 g, 87%) as a white solid material. $R_f$ = 0.3 (50% v/v acetone in $CH_2Cl_2$). Physical data for the mixture of rotamers (~4:6 by $^1$H NMR): MALDI-HRMS $m/z$ 579.0871 ([M + Na]$^+$, $C_{21}H_{19}F_3N_6O_7S{\cdot}Na^+$, calcd 579.0880); $^1$H NMR[31,32] (500 MHz, DMSO-$d_6$) $\delta$ 11.21 (s, 1H, ex, NH$_{A+B}$), 8.76 (s, 0.6H, H2$_B$), 8.75 (s, 0.4H, H2$_A$), 8.60 (s, 0.4H, H8$_A$), 8.56 (s, 0.6H, H8$_B$), 8.04 (d, 2H, $J$ = 7.7 Hz, Bz$_{A+B}$), 7.48−7.66 (m, 3H, Bz$_{A+B}$), 6.83 (d, 0.6H, $J$ = 1.4 Hz, H1′$_B$), 6.80 (d, 0.4H, $J$ = 1.4 Hz, H1′$_A$), 6.72 (d, 0.6H, ex, $J$ = 4.1 Hz, 3′-OH$_B$), 6.68 (d, 0.4H, ex, $J$ = 4.1 Hz, 3′-OH$_A$), 4.91 (br s, 0.4H, H2′$_A$), 4.82 (d, 0.6H, $J$ = 4.1 Hz, H3′$_B$), 4.76 (d, 0.4H, $J$ = 4.1 Hz, H3′$_A$), 4.70 (br s, 0.6H, H2′$_B$), 4.60−4.67 (m, 2H, H5′$_{A+B}$), 4.46 (d, 0.4H, $J$ = 10.3 Hz, H5″$_A$), 4.26 (d, 0.6H, $J$ = 11.7 Hz, H5″$_B$), 4.03 (d, 0.6H, $J$ = 10.3 Hz, H5″$_A$), 3.86 (d, 0.5H, $J$ = 11.7 Hz, H5″$_B$), 3.29 (s, 3H, $CH_3SO_2$); $^{13}$C NMR (125 MHz, DMSO-$d_6$) $\delta$ 165.5, 155.3 (q, $J$ = 36.6 Hz, $COCF_3$), 155.1 (q, $J$ = 36.6 Hz, $COCF_3$), 151.7 (C2$_{A/B}$), 151.6 (C2$_{A/B}$), 150.3, 150.2, 141.2 (C8$_B$), 141.0 (C8$_A$), 132.4 (Bz), 128.44 (Bz), 128.42 (Bz), 128.39 (Bz), 128.38 (Bz), 125.5, 125.3, 115.5 (q, $J$ = 288 Hz, $CF_3$), 115.2 (q, $J$ = 288 Hz, $CF_3$), 87.0, 85.8, 84.8 (C1′$_A$), 83.9 (C1′$_B$), 72.5 (C3′$_B$), 70.7 (C3′$_A$), 65.7 (C5′), 65.4 (C5′), 65.3 (C2′$_B$), 63.7 (C2′$_A$), 52.8 (C5″$_B$), 52.6 (C5″$_A$), 37.0 ($CH_3SO_2$); $^{19}$F NMR (376 MHz, DMSO-$d_6$) $\delta$ −71.1 ($CF_{3,B}$), −72.1 ($CF_{3,A}$).

**(1*S*,3*R*,4*S*,7*R*)-3-(6-*N*-Benzoyladenin-9-yl)-1-benzoyloxymethyl-7-hydroxy-5-trifluoroacetyl-2-oxa-5-azabicyclo[2.2.1]-heptane (13).** NaOBz (2.99 g, 20.8 mmol) and 15-crown-5 (2.07 mL, 10.4 mmol) were added to a solution of alcohol **12** (5.79 g, 10.4 mmol) in anhydrous DMF (100 mL). The reaction mixture was stirred first at 90 °C for 5 h and then at rt for an additional 18 h. The mixture was concentrated to near dryness and taken up in EtOAc and brine. The layers were separated, and the aqueous layer was extracted with EtOAc (4 × 200 mL). The combined organic layers were evaporated to near dryness, and the resulting residue was purified by silica gel column chromatography (0−3.5% v/v *i*-PrOH in $CHCl_3$) to afford O5′-benzoylated nucleoside **13** (5.05 g, 83%) as a white foam. $R_f$ = 0.4 (10% v/v *i*-PrOH in $CHCl_3$). Physical data for the mixture of rotamers (~4.5:5.5 by $^1$H NMR): MALDI-HRMS $m/z$ 605.1337 ([M + Na]$^+$, $C_{27}H_{21}F_3N_6O_6{\cdot}Na^+$ calcd 605.1367); $^1$H NMR[31,32] (500 MHz, DMSO-$d_6$) $\delta$ 11.21 (br s, 1H, ex, NH$_{A+B}$), 8.69 (s, 1H, H2$_{A+B}$), 8.59 (s, 0.45H, H8$_A$), 8.54 (s, 0.55H, H8$_B$), 8.05−8.13 (m, 4H, Bz$_{A+B}$), 7.49−7.72 (m, 6H, Bz$_{A+B}$), 6.86 (d, 0.55H, $J$ = 1.7 Hz, H1′$_B$), 6.83 (d, 0.45H, $J$ = 1.7 Hz, H1′$_A$), 6.60−6.80 (br s, 1H, ex, 3′-OH$_{A+B}$), 4.93 (s, 0.55 H, H3′$_B$), 4.89−4.91 (m, 0.9H, H2′$_A$, H3′$_A$), 4.74−4.79 (m, 1.0H, H5′$_{A+B}$), 4.68 (br s, 0.55H, H2′$_B$), 4.58−4.64 (m, 1.0H, H5′$_{A+B}$), 4.54 (d, 0.45H, $J$ = 10.7 Hz, H5″$_A$), 4.35 (d, 0.55H, $J$ = 11.5 Hz, H5″$_B$), 4.10 (d, 0.45H, $J$ = 10.7 Hz, H5″$_A$), 3.93 (d, 0.55H, $J$ = 11.5 Hz, H5″$_B$); $^{13}$C NMR (125 MHz, DMSO-$d_6$) $\delta$ 166.5, 165.3, 155.1 (2q, $J$ = 36 Hz, $COCF_3$), 151.8 (C2$_{A/B}$), 151.6 (C2$_{A/B}$), 151.4, 140.6 (C8$_{A/B}$), 140.4 (C8$_{A/B}$), 134.5, 134.4, 133.6 (Bz), 131.9 (Bz), 129.55 (Bz), 129.54 (Bz), 129.18, 129.17, 128.7 (Bz), 128.4 (Bz), 128.2 (Bz), 125.5, 125.3, 115.5 (2q, $CF_3$, $J$ = 286 MHz, $CF_3$), 87.4, 86.0, 84.5 (C1′$_A$), 83.7 (C1′$_B$), 72.9 (C3′$_B$), 71.0 (C3′$_A$), 65.3 (C2′$_B$), 63.7 (C2′$_A$), 60.7


dx.doi.org/10.1021/jo4022937 | J. Org. Chem. 2013, 78, 12690−12702

(C5′), 60.2 (C5′), 53.0 ($C5''_B$), 52.9 ($C5''_A$), minor impurities were observed at $\delta$ 121.3, 119.9, and 79.1; $^{19}$F NMR (376 MHz, DMSO-$d_6$) $\delta$ −71.1 ($CF_{3,B}$), −72.0 ($CF_{3,A}$).

**(1*S*,3*R*,4*S*,7*R*)-3-(6-*N*-Benzoyladenin-9-yl)-7-hydroxy-1-hydroxymethyl-2-oxa-5-azabicyclo[2.2.1]heptane (14).** From **13**: Aqueous NaOH (2 M, 17.5 mL, 0.35 mol) was added to an ice-cold solution of alcohol **13** (3.41 g, 5.85 mmol) in 1,4-dioxane and water (225 mL, 2:1 v/v). The reaction mixture was stirred at 0 °C for 2 h, at which point sat. aq. $NH_4Cl$ (25 mL) was added. The solution was evaporated to dryness, and the resulting crude material was adsorbed on silica gel and purified by silica gel column chromatography (0−20% v/v MeOH in $CH_2Cl_2$) to afford amino alcohol **14** (1.33 g, 60%) as a white solid material. $R_f$ = 0.4 (20% v/v MeOH in $CH_2Cl_2$); MALDI-HRMS *m*/*z* 405.1294 ([M + Na]$^+$, $C_{18}H_{18}N_6O_4{\cdot}Na^+$, calcd 405.1282); $^1$H NMR (300 MHz, DMSO-$d_6$) $\delta$ 11.17 (br s, 1H, ex, NH), 8.73 (s, 1H, $A^{Bz}$), 8.71 (s, 1H, $A^{Bz}$), 8.05 (d, 2H, *J* = 8.1 Hz, Bz), 7.49−7.67 (m, 3H, Bz), 6.44 (d, 1H, *J* = 1.9 Hz, H1′), 5.70 (d, 1H, ex, *J* = 4.0 Hz, 3′-OH), 4.82 (t, 1H, ex, *J* = 5.5 Hz, 5′-OH), 4.30 (d, 1H, *J* = 4.0 Hz, H3′), 3.69 (d, 2H, *J* = 5.5 Hz, H5′), 3.51 (s, 1H, H2′), 3.15−3.20 (d, 1H, *J* = 10.6 Hz, H5″), 2.94−3.01 (d, 1H, *J* = 10.6 Hz, H5″); $^{13}$C NMR (75.5 MHz, DMSO-$d_6$) $\delta$ 165.5, 152.0, 151.2, 149.8, 143.2, 133.3, 132.3, 128.4, 125.2, 91.3, 83.9, 73.4, 62.2 (C5″), 58.3 (C2′), 50.6 (C5′).

From **16**: Nucleoside **16** (1.00 g, 1.01 mmol) was dissolved in $CHCl_2COOH/MeOH/CH_3NO_2$ (50 mL, 3:5:92 v/v/v), and the solution was stirred at 0 °C for 15 min. Sat. aq. $NaHCO_3$ was carefully added to neutralize the solution, and the mixture was evaporated to dryness and adsorbed on silica gel. The resulting residue was purified by silica gel column chromatography (0−20% v/v MeOH in $CH_2Cl_2$, initially built including 1% v/v $Et_3N$) to afford amino diol **14** as a white solid material (0.37 g, 96%).

**(1*S*,3*R*,4*S*,7*R*)-3-(6-*N*-Benzoyladenin-9-yl)-1-(4,4′-dimethoxytrityloxymethyl)-7-hydroxy-2-oxa-5-azabicyclo[2.2.1]heptane (15) and (1*S*,3*R*,4*S*,7*R*)-3-(6-*N*-Benzoyladenin-9-yl)-5-(4,4′-dimethoxytrityl)-1-(4,4′-dimethoxytrityloxymethyl)-7-hydroxy-2-oxa-5-azabicyclo[2.2.1]heptane (16).** Amino alcohol **14** (1.25 g, 3.27 mmol) was coevaporated with anhydrous pyridine (30 mL) and redissolved in anhydrous pyridine (65 mL). The solution was cooled using an ice−salt mixture, and DMTrCl (1.55 g, 4.58 mmol) was added in one portion (addition over several portions did not influence reaction outcome). The reaction mixture was warmed to rt and stirred for 23 h, at which point MeOH (10 mL) was added. The mixture was diluted with EtOAc (100 mL) and washed with sat. aq. $NaHCO_3$ (2 × 15 mL). The combined aqueous layers were back-extracted with EtOAc (3 × 30 mL), and the combined organic phases were evaporated to dryness and subsequently coevaporated with abs. EtOH:toluene (3 × 50 mL, 2:1 v/v). The resulting residue was purified by silica gel column chromatography (0−8% v/v MeOH in $CH_2Cl_2$, initially built with 0.5% v/v $Et_3N$) and subsequently coevaporated with abs. EtOH:toluene (2 × 50 mL, 1:1 v/v) to afford nucleoside **15** (0.85 g, 38%) as a white solid material along with nucleoside **16** (0.97 g, 30%) as a yellow foam.

Physical data for **15**: $R_f$ = 0.4 (10% v/v MeOH in $CH_2Cl_2$); MALDI-HRMS *m*/*z* 707.2609 ([M + Na]$^+$, $C_{39}H_{36}N_6O_6{\cdot}Na^+$, calcd 707.2589); $^1$H NMR[31] (500 MHz, DMSO-$d_6$) $\delta$ 11.16 (br s, 1H, ex, NH), 8.78 (s, 1H, H8), 8.73 (s, 1H, H2), 8.06 (d, 2H, *J* = 7 Hz, Bz), 7.63−7.67 (t, 1H, *J* = 7.7 Hz, Bz), 7.54−7.58 (d, 2H, *J* = 7.0 Hz, Bz), 7.19−7.44 (m, 9H, DMTr), 6.86−6.92 (m, 4H, DMTr), 6.54 (d, 1H, *J* = 1.9 Hz, H1′), 5.66 (d, 1H, ex, *J* = 4.8 Hz, 3′-OH), 4.40 (d, 1H, *J* = 4.8 Hz, H3′), 3.74 (s, 6H, $CH_3O$), 3.50 (br s, 1H, H2′), 3.30−3.32 (m, 1H, H5′, overlap with $H_2O$), 3.25−3.27 (d, 1H, *J* = 10.7 Hz, H5′), 3.19 (br s, 2H, H5″), 2.90 (br s, 1H, ex, 2′-NH); $^{13}$C NMR (125 MHz, DMSO-$d_6$) $\delta$ 165.5, 158.0, 152.2, 151.3 (C2), 149.9, 144.8, 143.3 (C8), 135.5, 135.4, 133.4, 132.3 (Ar), 129.71 (Ar), 129.68 (Ar), 128.45, 128.39 (Ar), 127.8 (Ar), 127.7 (Ar), 126.6 (Ar), 125.2, 113.2 (DMTr), 89.6, 85.1, 84.1 (C1′), 74.0 (C3′), 62.2 (C2′), 61.2 (C5′), 55.0 ($CH_3O$), 51.2 (C5″).

Physical data for **16**: $R_f$ = 0.5 (3% v/v MeOH in $CH_2Cl_2$); MALDI-HRMS *m*/*z* 1009.3900 ([M + Na]$^+$, $C_{60}H_{54}N_6O_8{\cdot}Na^+$, calcd 1009.3895); $^1$H NMR[31] (500 MHz, DMSO-$d_6$) $\delta$ 11.33 (br s, 1H, ex, NH), 9.13 (s, 1H, H8), 8.77 (s, 1H, H2), 8.10 (d, 2H, *J* = 7.5 Hz, Bz), 7.64−7.67 (t, 1H, *J* = 7.5 Hz, Bz), 7.52−7.58 (t, 2H, *J* = 7.5 Hz, Bz), 6.78−7.41 (m, 22H, DMTr), 6.58 (d, 1H, *J* = 1.1 Hz, H1′), 6.53 (d, 2H, *J* = 9.1 Hz, DMTr), 6.43 (d, 2H, *J* = 9.1 Hz, DMTr), 4.26 (d, 1H, *J* = 5.0 Hz, H3′), 3.82 (d, 1H, *J* = 9.9 Hz, H5″), 3.75 (br s, 1H, H2′), 3.73 (s, 6H, $CH_3O$), 3.65 (s, 3H, $CH_3O$), 3.62 (s, 3H, $CH_3O$), 3.55 (d, 1H, ex, *J* = 5.0 Hz, 3′-OH), 3.17−3.19 (d, 1H, *J* = 11.0 Hz, H5′), 3.09−3.11 (d, 1H, *J* = 11.0 Hz, H5′), 2.98 (d, 1H, *J* = 9.9 Hz, H5″); $^{13}$C NMR (125 MHz, DMSO-$d_6$) $\delta$ 165.7, 158.0, 157.05, 156.96, 152.0, 151.6 (C2), 150.3, 145.2, 144.8, 142.9 (C8), 136.7, 136.2, 136.0, 135.4, 135.3, 133.3, 132.4 (Bz), 130.5 (DMTr), 130.2 (DMTr), 129.8 (DMTr), 129.7 (DMTr), 128.8 (DMTr), 128.44 (Bz), 128.39 (Bz), 127.73 (DMTr), 127.70 (DMTr), 127.1 (DMTr), 126.5 (DMTr), 126.3, 125.5 (DMTr), 123.8 (DMTr), 113.1 (DMTr), 112.5 (DMTr), 112.4 (DMTr), 88.4, 86.6 (C1′), 85.2, 74.3, 74.0 (C3′), 64.3 (C2′), 60.7 (C5′), 55.0 (C5″), 54.9 ($CH_3O$), 54.8 ($CH_3O$), 54.75 ($CH_3O$), 54.73 ($CH_3O$). A trace impurity of pyridine was identified in the $^{13}$C NMR spectrum at $\delta$ 149.5.

**(1*S*,3*R*,4*S*,7*R*)-3-(6-*N*-Benzoyladenin-9-yl)-1-(4,4′-dimethoxytrityloxymethyl)-5-(9′-fluorenylmethoxycarbonyl)-7-hydroxy-2-oxa-5-azabicyclo[2.2.1]heptane (17).** Amino alcohol **15** (200 mg, 0.29 mmol) was coevaporated in anhydrous pyridine (2 × 2 mL) and redissolved in anhydrous pyridine (1.5 mL). The solution was cooled to 0 °C, and 9′-fluorenylmethyl chloroformate (100 mg, 0.38 mmol) added thereto. The reaction mixture was warmed to rt and stirred for 6 h, at which point it was diluted with EtOAc (30 mL) and washed with sat. aq. $NaHCO_3$ (30 mL). The aqueous layer was back-extracted with EtOAc (25 mL), and the combined organic layers were evaporated to near dryness. The resulting crude material was coevaporated with abs. EtOH:toluene (2 × 6 mL, 2:1 v/v) and purified by silica gel column chromatography (30−100% v/v EtOAc in petroleum ether) to afford target nucleoside **17** (136 mg, 51%) as a white foam. $R_f$ = 0.4 (EtOAc). Physical data for the mixture of rotamers (∼1:1.2 by $^1$H NMR): MALDI-HRMS *m*/*z* 929.3241 ([M + Na]$^+$, $C_{54}H_{46}N_6O_8{\cdot}Na^+$, calcd 929.3269); $^1$H NMR (300 MHz, DMSO-$d_6$) $\delta$ 11.29 (br s, ex), 8.74 (s, 1H), 8.72 (s, 1.2H), 8.55 (s, 1.2H), 8.49 (s, 1H), 6.90−8.08 (m, 57.2H), 6.80 (d, 1.2H, *J* = 1.7 Hz), 6.73 (d, 1H, *J* = 1.7 Hz), 6.25 (d, 1.2H, ex, *J* = 4.4 Hz), 6.22 (d, 1H, ex, *J* = 4.4 Hz), 4.50 (br s, 1.2H), 4.45 (br s, 1H), 4.22 (d, 1H, *J* = 6.9 Hz), 4.15 (d, 1.2H, *J* = 6.9 Hz), 3.87 (d, 1H, *J* = 6.9 Hz), 3.83 (d, 1.2H, *J* = 6.9 Hz), 3.62−3.76 (m, 17.6H), 3.34−3.43 (m, 6.6H); $^{13}$C NMR (75.5 MHz, DMSO-$d_6$) $\delta$ 165.66, 165.63, 158.1, 154.7, 154.6, 151.8, 151.5, 150.3, 150.2, 144.7, 143.7, 143.6, 143.5, 142.8, 141.3, 141.2, 140.6, 140.4, 140.3, 135.3, 135.2, 133.3, 132.4, 129.7, 128.8, 128.4, 127.9, 127.7, 127.6, 127.5, 127.2, 127.1, 126.9, 126.7, 125.4, 125.2, 125.1, 124.9, 124.6, 121.3, 119.98, 113.2, 88.9, 88.4, 85.4, 84.9, 84.7, 84.6, 72.5, 72.1, 66.8, 66.7, 63.9, 63.4, 60.6, 60.5, 55.0, 52.7, 52.6, 46.4, 45.9.

**(1*S*,3*R*,4*S*,7*R*)-3-(6-*N*-Benzoyladenin-9-yl)-1-(4,4′-dimethoxytrityloxymethyl)-7-hydroxy-5-(pyren-1-yl)methyl-2-oxa-5-azabicyclo[2.2.1]heptane (18).** Nucleoside **15** (225 mg, 0.33 mmol) was coevaporated with anhydrous 1,2-dichloroethane (2 × 5 mL) and redissolved in anhydrous 1,2-dichloroethane (4 mL). 1-Pyrenecarboxaldehyde (115 mg, 0.49 mmol) and $NaBH(OAc)_3$ (104 mg, 0.49 mmol) were added, and the resulting suspension was stirred at rt for 17 h, at which point sat. aq. $NaHCO_3$ (30 mL) was added. The mixture was extracted with $CH_2Cl_2$ (3 × 15 mL), and the combined organic layers were dried ($Na_2SO_4$) and evaporated to dryness. The resulting residue was purified by silica gel column chromatography (0−5% v/v MeOH in $CH_2Cl_2$) to afford N2′-alkylated nucleoside **18** as a white foam (201 mg, 68%). $R_f$ = 0.4 (EtOAc); MALDI-HRMS *m*/*z* 921.3326 ([M + Na]$^+$, $C_{56}H_{46}N_6O_6{\cdot}Na^+$, calcd 921.3371); $^1$H NMR[31] (500 MHz, DMSO-$d_6$) $\delta$ 11.18 (s, 1H, ex, NH), 8.53 (s, 1H, H2), 8.46 (s, 1H, H8), 7.97−8.24 (m, 8H, Ar), 7.60−7.85 (m, 6H, Ar), 7.41−7.44 (m, 2H, DMTr), 7.19−7.32 (m, 7H, DMTr), 6.85−6.92 (m, 4H, DMTr), 6.50 (d, 1H, *J* = 1.9 Hz, H1′), 6.14 (d, 1H, ex, *J* = 3.6 Hz, 3′-OH), 4.72−4.75 (d, 1H, *J* = 12.5 Hz, $CH_2Py$), 4.60 (d, 1H, *J* = 3.6 Hz, H3′), 4.52−4.56 (d, 1H, *J* = 12.5 Hz, $CH_2Py$), 3.73 (s, 6H, $CH_3O$), 3.66 (s, 1H, H2′), 3.34−3.45 (m, 3H, 2 × H5′, H5″), 3.17−3.20 (d, 1H, *J* = 10.3 Hz, H5″); $^{13}$C NMR (125 MHz, DMSO-$d_6$) $\delta$ 165.6, 158.0, 151.7, 151.0 (C2), 149.9, 144.8,


dx.doi.org/10.1021/jo4022937 | J. Org. Chem. 2013, 78, 12690−12702

142.8 (C8), 135.5, 135.4, 133.6, 133.2, 132.4 (Ar), 130.6, 130.2, 130.0, 129.71 (DMTr), 129.68 (DMTr), 128.7, 128.5 (Ar), 128.4 (Ar), 127.8 (DMTr), 127.7 (DMTr), 127.6 (Ar), 127.2 (Ar), 126.9 (Ar), 126.8 (Ar), 126.6 (DMTr), 125.9 (Ar), 125.5, 124.9 (Ar), 124.8 (Ar), 124.2 (Ar), 123.9, 123.7, 123.1 (Ar), 113.2 (DMTr), 90.3, 85.2, 84.8 (C1′), 75.4 (C3′), 66.3 (C2′), 61.3 (C5′), 59.2 (C5″), 58.2 ($CH_2Py$), 55.0 ($CH_3O$).

**(1*S*,3*R*,4*S*,7*R*)-3-(6-*N*-Benzoyladenin-9-yl)-1-(4,4′-dimethoxytrityloxymethyl)-7-hydroxy-5-(pyren-1-yl)carbonyl-2-oxa-5-azabicyclo[2.2.1]heptane (19).** Amino alcohol **15** (0.41 g, 0.59 mmol) was coevaporated with anhydrous 1,2-dichloroethane (2 × 10 mL) and dissolved in anhydrous $CH_2Cl_2$ (11.9 mL), and 1-ethyl-3-(3-dimethylaminopropyl)carbodiimide hydrochloride (EDC·HCl) (226 mg, 1.19 mmol) and 1-pyrenecarboxylic acid (0.29 g, 1.19 mmol) were added thereto. The reaction mixture was stirred for 45 h at rt, at which point it was diluted with $CH_2Cl_2$ (50 mL) and washed with water (20 mL). The two phases were separated, and the aqueous phase was back-extracted with $CH_2Cl_2$ (3 × 50 mL). The combined organic phases were evaporated to dryness, and the resulting residue was purified by silica gel column chromatography (0−99% v/v EtOAc and 1% v/v pyridine in petroleum ether). The resulting product was coevaporated with abs. EtOH:toluene (2 × 50 mL, 1:1 v/v) to afford nucleoside **19** (343 mg, 64%) as a yellow solid material. Physical data for the mixture of rotamers (∼0.4:1 by $^1$H NMR): $R_f$ = 0.5 (5% v/v MeOH:$CH_2Cl_2$); MALDI-HRMS *m*/*z* 935.3138 ([M + Na]$^+$, $C_{56}H_{44}N_6O_7$·Na$^+$, calcd 935.3164). $^1$H NMR[31,32] (300 MHz, DMSO-$d_6$) $\delta$ 11.21 (br s, 1.4H, ex, NH), 8.55 (s, 1H, $A^{Bz}{}_B$), 8.53 (s, 0.4H, $A^{Bz}{}_A$), 8.45 (s, 1H, $A^{Bz}{}_B$), 8.40 (s, 0.4H, $A^{Bz}{}_A$), 6.82−8.23 (m, ∼37.8H, $Ar_{A+B}$), 6.50 (d, 1H, *J* = 2.2 Hz, H1′$_B$), 6.40 (d, 0.4H, *J* = 1.8 Hz, H1′$_A$), 6.15 (d, 1H, ex, *J* = 4.0 Hz, 3′-$OH_B$), 6.07 (d, 0.4H, ex, *J* = 3.7 Hz, 3′-$OH_A$), 4.42−4.77 (m, 4.2H, H3′$_{A+B}$, H5′$_{A+B}$), 3.55−3.75 (m, ∼9.8H, $CH_3O_{A+B}$, H2′$_{A+B}$), 3.15−3.44 (m, ∼2.8H, H5″$_{A+B}$); $^{13}$C NMR (75.5 MHz, DMSO-$d_6$) $\delta$ 165.5, 157.9, 157.7, 151.7, 150.98, 149.8, 148.2, 144.7, 142.8, 140.1, 135.4, 135.3, 133.5, 133.1, 132.3, 130.5, 130.2, 129.9, 129.6, 128.8, 128.6, 128.4, 127.8, 127.6, 127.5, 127.3, 127.2, 126.9, 126.5, 126.3, 125.9, 125.5, 124.9, 124.8, 124.78, 124.2, 123.8, 123.7, 123.1, 113.1, 112.7, 92.0, 90.3, 85.1, 84.7, 79.8, 75.3, 74.7, 66.4, 61.2, 59.1, 58.6, 58.3, 58.2, 54.6.

**(1*S*,3*R*,4*S*,7*R*)-3-(6-*N*-Benzoyladenin-9-yl)-1-(4,4′-dimethoxytrityloxymethyl)-7-hydroxy-5-(pyren-1-yl)acetyl-2-oxa-5-azabicyclo[2.2.1]heptane (20).** Amino alcohol **15** (0.25 g, 0.37 mmol) was coevaporated with anhydrous 1,2-dichloroethane (2 × 5 mL) and dissolved in anhydrous $CH_2Cl_2$ (10 mL). To this was added 1-ethyl-3-(3-dimethylaminopropyl)carbodiimide hydrochloride (EDC·HCl) (108 mg, 0.55 mmol) and 1-pyreneacetic acid (145 mg, 0.55 mmol). The reaction mixture was stirred for 2.5 h at rt, at which point it was diluted with $CH_2Cl_2$ (20 mL) and washed with water (2 × 10 mL). The aqueous layer was back-extracted with $CH_2Cl_2$ (10 mL), and the combined organic layers were evaporated to dryness. The resulting crude residue was purified by silica gel column chromatography (0−4% v/v MeOH in $CH_2Cl_2$) to afford nucleoside **20** as a white solid (0.27 g, 79%). Physical data for the mixture of rotamers (∼0.5:1.0 by $^1$H NMR): $R_f$ = 0.5 (10% v/v MeOH:$CH_2Cl_2$); MALDI-HRMS *m*/*z* 949.3321 ([M + Na]$^+$, $C_{57}H_{46}N_6O_7$·Na$^+$, calcd 949.3320); $^1$H NMR[31,32] (500 MHz, DMSO-$d_6$) $\delta$ 11.29 (br s, 1.5H, ex, $NH_{A+B}$), 8.97 (s, 1H, $H8_B$), 8.73 (s, 0.5H, $H2_A$), 8.71 (s, 1H, $H2_B$), 8.55 (s, 0.5H, $H8_A$), 6.91−8.32 (m, 40.5H, $Ar_{A+B}$), 6.83 (d, 0.5H, *J* = 1.7 Hz, H1′$_A$), 6.80 (d, 1H, *J* = 1.4 Hz, H1′$_B$), 6.32 (d, 0.5H, ex, *J* = 4.4 Hz, 3′-$OH_A$), 6.19 (d, 1H, ex, *J* = 4.4 Hz, 3′-$OH_B$), 5.07 (s, 0.5H, H2′$_A$), 4.71−4.73 (m, 1.5H, H2′$_B$, H3′$_A$), 4.67 (d, 1H, *J* = 10.4 Hz, H5″$_B$), 4.63 (d, 1H, *J* = 4.4 Hz, H3′$_B$), 4.55−4.60 (d, 1H, *J* = 17.0 Hz, $CH_2Py_B$), 4.36−4.40 (d, 1H, *J* = 17.0 Hz, $CH_2Py_B$), 4.11 (d, 0.5H, *J* = 16.2 Hz, $CH_2Py_A$), 3.96−4.03 (m, 1.5H, H5″$_A$, H5″$_B$), 3.66−3.77 (m, 9.5H, $CH_3O$, H5″$_A$), 3.34−3.48 (m, 3.5H, H5′$_{A+B}$, $CH_2Py_A$); $^{13}$C NMR (125 MHz, DMSO-$d_6$) $\delta$ 169.9, 169.6, 165.6, 165.5, 158.1, 158.0, 152.0, 151.7 ($A^{Bz}{}_A$), 151.5, 151.4 ($A^{Bz}{}_B$), 150.6, 150.2, 144.71, 144.68, 141.7 ($A^{Bz}{}_B$), 141.5 ($A^{Bz}{}_A$), 135.4, 135.2, 133.54, 133.47, 132.5 (Ar), 130.70, 130.69, 130.28, 130.1, 129.91, 129.88, 129.82 (Ar), 129.79 (Ar), 129.77, 129.74 (Ar), 129.68, 129.62, 129.4, 129.2, 128.8, 128.7, 128.58 (Ar), 128.56 (Ar), 128.54 (Ar), 128.46 (Ar), 128.2 (Ar), 127.85 (Ar), 127.77 (Ar), 127.72 (Ar), 127.4 (Ar), 127.27 (Ar), 127.2 (Ar), 127.1 (Ar), 126.9, 126.8 (Ar), 126.68 (Ar), 126.2, 126.0 (Ar), 125.9 (Ar), 125.4, 125.3, 125.00 (Ar), 124.98 (Ar), 124.82 (Ar), 124.76 (Ar), 124.7 (Ar), 124.6 (Ar), 124.5 (Ar), 124.4 (Ar), 124.3 (Ar), 124.1, 123.89, 123.79, 123.76, 123.72, 123.2 (Ar), 113.2 (Ar), 89.0, 88.4, 85.5, 85.4, 84.73 (C1′$_A$), 84.66 (C1′$_B$), 72.9 (C3′$_A$), 72.0 (C3′$_B$), 64.5 (C2′$_A$), 61.8 (C2′$_B$), 60.9 (C5′$_B$), 60.8 (C5′$_A$), 55.0 ($CH_3O$), 52.8 (C5″$_B$), 52.3 (C5″$_A$), 37.8 ($CH_2Py_B$), 37.7 ($CH_2Py_A$). Trace impurities of dichloromethane and 1-pyreneacetic acid were identified in the $^{13}$C NMR spectrum. The compound was used in the next step without further purification.

**(1*S*,3*R*,4*S*,7*R*)-3-(6-*N*-Benzoyladenin-9-yl)-7-[2-cyanoethoxy-(diisopropylamino)phosphinoxy]-1-(4,4′-dimethoxytrityloxymethyl)-5-(9″-fluorenylmethoxycarbonyl)-2-oxa-5-azabicyclo-[2.2.1]heptane (1).** Nucleoside **17** (225 mg, 0.25 mmol) was coevaporated with anhydrous 1,2-dichloroethane (2 × 4 mL) and redissolved in anhydrous $CH_2Cl_2$ (3.5 mL). Anhydrous *N*,*N*′-diisopropylethylamine (DIPEA) (195 $\mu$L, 1.12 mmol) and *N*-methylimidazole (NMI) (16 $\mu$L, 0.20 mmol) were added, followed by dropwise addition of 2-cyanoethyl-*N*,*N*′-diisopropylchlorophosphoramidite (111 $\mu$L, 0.50 mmol). The reaction mixture was stirred for 4 h at rt and evaporated to dryness, and the resulting residue was purified by silica gel column chromatography (0−2% v/v MeOH in $CH_2Cl_2$ v/v, initially built in 0.5% v/v $Et_3N$) and subsequent precipitation from $CH_2Cl_2$/petroleum ether to afford target amidite **1** (126 mg, 46%) as a white foam. Physical data for mixture of rotamers: $R_f$ = 0.5 (5% v/v MeOH in $CH_2Cl_2$); ESI-HRMS *m*/*z* 1129.4356 ([M + Na]$^+$, $C_{63}H_{63}N_8O_9P$·Na$^+$, calcd 1129.4348); $^{31}$P NMR (121 MHz, $CDCl_3$) $\delta$ 150.32, 150.26, 150.1, 149.5.

**(1*S*,3*R*,4*S*,7*R*)-3-(6-*N*-Benzoyladenin-9-yl)-7-[2-cyanoethoxy-(diisopropylamino)phosphinoxy]-1-(4,4′-dimethoxytrityloxymethyl)-5-(pyren-1-yl)methyl-2-oxa-5-azabicyclo[2.2.1]-heptane (2).** Nucleoside **18** (155 mg, 0.17 mmol) was coevaporated with 1,2-dichloroethane (2 × 5 mL) and dissolved in a 20% v/v *N*,*N*′-diisopropylethylamine solution in anhydrous $CH_2Cl_2$ (5.0 mL). To this was added 2-cyanoethyl-*N*,*N*′-diisopropylchlorophosphoramidite (0.10 mL, 0.44 mmol), and the reaction mixture was stirred at rt for 17 h, whereupon the reaction was quenched with abs EtOH (1 mL) and the mixture was evaporated to dryness. The resulting residue was purified by silica gel column chromatography (0−90% v/v EtOAc in petroleum ether) and precipitated from $CH_2Cl_2$/petroleum ether to afford amidite **2** as a white solid material (131 mg, 69%). $R_f$ = 0.7 (5% v/v MeOH in $CH_2Cl_2$); ESI-HRMS *m*/*z* 1099.4642 ([M + H]$^+$, $C_{65}H_{63}N_8O_7P$·H$^+$, calcd 1099.4630); $^{31}$P NMR (121 MHz, $CDCl_3$) $\delta$ 150.6, 148.4.

**(1*S*,3*R*,4*S*,7*R*)-3-(6-*N*-Benzoyladenin-9-yl)-7-[2-cyanoethoxy-(diisopropylamino)phosphinoxy]-1-(4,4′-dimethoxytrityloxymethyl)-5-(pyren-1-yl)carbonyl-2-oxa-5-azabicyclo[2.2.1]-heptane (3).** Nucleoside **19** (0.30 g, 0.33 mmol) was coevaporated with 1,2-dichloroethane (2 × 5 mL) and dissolved in 20% v/v *N*,*N*′-diisopropylethylamine in anhydrous $CH_2Cl_2$ (3.4 mL). To this was added 2-cyanoethyl-*N*,*N*′-diisopropylchlorophosphoramidite (0.11 mL, 0.49 mmol), and the reaction mixture was stirred for 22 h at rt, at which point abs. EtOH (2 mL) was added. The mixture was taken up in $CH_2Cl_2$ (50 mL) and washed with sat. aq. $NaHCO_3$ (50 mL) and brine (50 mL). The combined aqueous layers were back-extracted with $CH_2Cl_2$ (2 × 20 mL), and the combined organic layers were evaporated to dryness. The resulting residue was purified by silica gel column chromatography (0−99% v/v EtOAc in petroleum ether containing 1% v/v pyridine), coevaporated with abs. EtOH:toluene (2 × 50 mL, 1:1 v/v), and precipitated from EtOAc/hexane to afford phosphoramidite **3** as a white foam (247 mg, 67%). Physical data for the mixture of rotamers: $R_f$ = 0.5 (EtOAc); ESI-HRMS *m*/*z* 1113.4462 ([M + H]$^+$, $C_{65}H_{61}N_8O_8P$·H$^+$, calcd 1113.4422); $^{31}$P NMR (121 MHz, $CDCl_3$) $\delta$ 152.3, 151.8, 150.2.

**(1*S*,3*R*,4*S*,7*R*)-3-(6-*N*-Benzoyladenin-9-yl)-7-[2-cyanoethoxy-(diisopropylamino)phosphinoxy]-1-(4,4′-dimethoxytrityloxymethyl)-5-(pyren-1-yl)acetyl-2-oxa-5-azabicyclo[2.2.1]heptane (4).** Nucleoside **20** (235 mg, 0.25 mmol) was coevaporated with anhydrous 1,2-dichloroethane (2 × 5 mL) and redissolved in anhydrous $CH_2Cl_2$ (5 mL). Anhydrous *N*,*N*′-diisopropylethylamine


dx.doi.org/10.1021/jo4022937 | J. Org. Chem. 2013, 78, 12690−12702

(220 μL, 1.27 mmol) was added, followed by dropwise addition of 2-cyanoethyl-*N*,*N*′-diisopropylchlorophosphoramidite (115 μL, 0.51 mmol). The reaction mixture was stirred at rt for 22 h, at which point abs. EtOH (1 mL) was added. The solution was evaporated to dryness, and the resulting crude residue was purified by silica gel column chromatography (0−2% v/v MeOH in $CH_2Cl_2$) and precipitation from $CH_2Cl_2$/petroleum ether to afford target amidite **4** (203 mg, 71%) as a white foam. Physical data for the mixture of rotamers: $R_f$ = 0.6 (5% v/v MeOH in $CH_2Cl_2$); MALDI-HRMS *m*/*z* 1149.4358 ($[M + Na]^+$, $C_{66}H_{63}N_8O_8P{\cdot}Na^+$, calcd 1149.4399); $^{31}P$ NMR (121 MHz, $CDCl_3$) δ 150.4, 150.31, 150.26, 148.1.

**Synthesis of ONs.** **W**/**X**/**Y**/**Z**-modified oligodeoxyribonucleotides were made on an automated DNA synthesizer using 0.2 μmol scale succinyl-linked long-chain alkylamine controlled pore glass (LCAA-CPG) columns with a pore size of 500 Å. Phosphoramidites **1**−**4** were incorporated into ONs using the following hand-coupling conditions (activator; coupling time; stepwise coupling yield): monomer **W** (pyridinium hydrochloride; 30 min; ∼82%); monomers **X**−**Z** (pyridinium hydrochloride; 15 min; ∼95%). Standard protocols for incorporation of DNA phosphoramidites were used. Modified ONs were deprotected using 32% aq. $NH_3$ (55 °C, 2−12 h) and purified (DMTr-ON) by ion-pair reversed-phase HPLC using either an ammonium formate/acetonitrile gradient or a triethylammonium acetate/acetonitrile gradient, which was followed by detritylation (80% aq. AcOH, 20 min) and precipitation (abs. EtOH or acetone, −18 °C, 12 h). The compositions of the modified ONs were verified by MALDI-MS analysis (Tables S1 and S2 in the Supporting Information) recorded in either positive or negative ion mode on a quadrupole time-of-flight tandem mass spectrometer equipped with a MALDI source using 3-hydroxypicolinic acid as a matrix. Purity (>90% unless stated otherwise) was verified either by the ion-pair reversed-phase HPLC system running in analytical mode or ion-exchange HPLC using a Tris-Cl/EDTA−NaCl gradient.

**Protocol for Thermal Denaturation Studies.** Concentrations of ONs were calculated using the following extinction coefficients ($OD_{260}$/μmol): G, 12.0; A, 15.2; T, 8.4; U, 10.0; C, 7.1; pyrene, 22.4. ONs (each strand at 1.0 μM) were thoroughly mixed, denatured by heating, and subsequently cooled to the starting temperature of the experiment. Quartz optical cells with a path length of 10.0 mm were used. The thermal denaturation temperature ($T_m$/°C) was measured on a temperature-controlled UV−vis spectrophotometer and determined as the maximum of the first derivative of the thermal denaturation curve ($A_{260}$ vs $T$) recorded in medium-salt buffer ($T_m$ buffer) (100 mM NaCl, 0.1 mM EDTA, and pH 7.0 adjusted with 10 mM $NaH_2PO_4$/5 mM $Na_2HPO_4$). The temperature of the denaturation experiments ranged from at least 15 °C below $T_m$ to 20 °C above $T_m$ (although not below 3 °C). A temperature ramp of 0.5 °C/min or 1.0 °C/min was used in the experiments. The reported thermal denaturation temperatures are averages of two measurements within ±1.0 °C.

**Protocol for UV−Vis Absorption Spectroscopy.** UV−vis spectra were recorded on a spectrophotometer at 5 °C (except for single-stranded **X**/**Y**-modified probes, which were recorded at room temperature) using each strand at a concentration of 1 μM in $T_m$ buffer and quartz cells with 1 cm path lengths.

**Protocol for Fluorescence Emission Spectroscopy.** Steady-state fluorescence spectra were recorded at 5 °C using an excitation wavelength of $\lambda_{ex}$ = 350 nm, each strand at 1 μM concentration in $T_m$ buffer (except with **Y**-modified ONs, where strands were used at 0.15 μM concentration), and quartz cells with 1 cm path lengths.

## ■ ASSOCIATED CONTENT

### Supporting Information

General experimental section; additional synthetic strategies; NMR spectra for all new compounds; MS data for all modified ONs; representative thermal denaturation curves; additional $T_m$ data; representative absorption and fluorescence emission spectra; and evaluation of SNP-discriminatory potential. This material is available free of charge via the Internet at http://pubs.acs.org.

## ■ AUTHOR INFORMATION


### Corresponding Author

*E-mail: hrdlicka@uidaho.edu.

### Author Contributions

§N.K.A. and B.A.A contributed equally.


### Notes

The authors declare no competing financial interest.

## ■ ACKNOWLEDGMENTS

P.J.H. appreciates financial support through Award R01 GM088697 from the National Institute of General Medical Sciences, National Institutes of Health, and from the Institute of Translational Health Sciences (ITHS) (supported by Grants UL1 RR025014, KL2 RR025015, and TL1 RR025016 from the National Center for Research Resources, NIH). J.W. appreciates financial support from The Danish National Research Foundation and the Danish Agency for Science Technology and Innovation. We thank Dr. T. Santhosh Kumar (University of Southern Denmark) for providing us with starting material and Dr. Lee Deobald (EBI Murdock Mass Spectrometry Center, University of Idaho) for mass spectrometric analyses.

## ■ REFERENCES


(1) For reviews of conformationally restricted nucleotides, see, for example: (a) Leumann, C. J. *Bioorg. Med. Chem.* **2002**, *10*, 841−854. (b) Obika, S.; Abdur Rahman, S. M.; Fujisaka, A.; Kawada, Y.; Baba, T.; Imanishi, T. *Heterocycles* **2010**, *81*, 1347−1392. (c) Prakash, T. P. *Chem. Biodiversity* **2011**, *8*, 1616−1641. (d) Deleavey, G. F.; Damha, M. J. *Chem. Biol.* **2012**, *19*, 937−954. (e) Zhou, C.; Chattopadhyaya, J. *Chem. Rev.* **2012**, *112*, 3808−3832.

(2) (a) Duca, M.; Vekhoff, P.; Oussedik, K.; Halby, L.; Arimondo, P. B. *Nucleic Acids Res.* **2008**, *36*, 5123−5138. (b) Bennett, C. F.; Swayze, E. E. *Annu. Rev. Pharmacol. Toxicol.* **2010**, *50*, 259−293. (c) Østergaard, M. E.; Hrdlicka, P. J. *Chem. Soc. Rev.* **2011**, *40*, 5771−5788. (d) Watts, J. K.; Corey, D. R. *J. Pathol.* **2012**, *226*, 365−379. (e) Matsui, M.; Corey, D. R. *Drug Discovery Today* **2012**, *17*, 443−450. (f) Dong, H.; Lei, J.; Ding, L.; Wen, Y.; Ju, H.; Zhang, X. *Chem. Rev.* **2013**, *113*, 6207−6233.

(3) Singh, S. K.; Nielsen, P.; Koshkin, A. A.; Wengel, J. *Chem. Commun.* **1998**, 455−456.

(4) Obika, S.; Nanbu, D.; Hari, Y.; Andoh, J.-I.; Morio, K.-I.; Doi, T.; Imanishi, T. *Tetrahedron Lett.* **1998**, *39*, 5401−5404.

(5) Kaur, H.; Babu, B. R.; Maiti, S. *Chem. Rev.* **2007**, *107*, 4672−4697.

(6) (a) Rajwanshi, V. K.; Håkansson, A. E.; Dahl, B. M.; Wengel, J. *Chem. Commun.* **1999**, 1395−1396. (b) Sørensen, M. D.; Kværnø, L.; Bryld, T.; Håkansson, A. E.; Verbeure, B.; Gaubert, G.; Herdewijn, P.; Wengel, J. *J. Am. Chem. Soc.* **2002**, *124*, 2164−2176.

(7) Recent examples include: (a) Seth, P. P.; Vasquez, G.; Allerson, C. A.; Berdeja, A.; Gaus, H.; Kinberger, G. A.; Prakash, T. P.; Migawa, M. T.; Bhat, B.; Swayze, E. E. *J. Org. Chem.* **2010**, *75*, 1569−1581. (b) Li, Q.; Yuan, F.; Zhou, C.; Plashkevych, O.; Chattopadhyaya, J. *J. Org. Chem.* **2010**, *75*, 6122−6140. (c) Liu, Y.; Xu, J.; Karimiahmadabadi, M.; Zhou, C.; Chattopadhyaya, J. *J. Org. Chem.* **2010**, *75*, 7112−7128. (d) Upadhayaya, R.; Deshpande, S. A.; Li, Q.; Kardile, R. A.; Sayyed, A. Y.; Kshirsagar, E. K.; Salunke, R. V.; Dixit, S. S.; Zhou, C.; Foldesi, A.; Chattopadhyaya, J. *J. Org. Chem.* **2011**, *76*, 4408−4431. (e) Shrestha, A. R.; Hari, Y.; Yahara, A.; Osawa, T.; Obika, S. *J. Org. Chem.* **2011**, *76*, 9891−9899. (f) Hanessian, S.; Schroeder, B. R.; Giacometti, R. D.; Merner, B. L.; Østergaard, M. E.; Swayze, E. E.; Seth, P. P. *Angew. Chem., Int. Ed.* **2012**, *51*, 11242−11245. (g) Haziri, A. I.; Leumann, C. J. *J. Org. Chem.* **2012**, *77*, 5861−

5869. (h) Gerber, A.-B.; Leumann, C. J. *Chem.—Eur. J.* **2013**, *19*, 6990−7006. (i) Morihiro, K.; Kodama, T.; Kentefu; Moai, Y.; Veedu, R. N.; Obika, S. *Angew. Chem., Int. Ed.* **2013**, *52*, 5074−5078. (j) Hari, Y.; Osawa, T.; Kotobuki, Y.; Yahara, A.; Shrestha, A. R.; Obika, S. *Bioorg. Med. Chem.* **2013**, *21*, 4405−4412. (k) Hari, Y.; Morikawa, T.; Osawa, T.; Obika, S. *Org. Lett.* **2013**, *15*, 3702−3705. (l) Migawa, M. T.; Prakash, T. P.; Vasquez, G.; Seth, P. P.; Swayze, E. E. *Org. Lett.* **2013**, *15*, 4316−4319. (m) Hanessian, S.; Schroeder, B. R.; Merner, B. L.; Chen, B.; Swayze, E. E.; Seth, P. P. *J. Org. Chem.* **2013**, *78*, 9051−9063. (n) Hanessian, S.; Wagger, J.; Merner, B. L.; Giacometti, R. D.; Østergaard, M. E.; Swayze, E. E.; Seth, P. P. *J. Org. Chem.* **2013**, *78*, 9064−9075.

(8) For recent examples, see: (a) Karmakar, S.; Anderson, B. A.; Rathje, R. L.; Andersen, S.; Jensen, T.; Nielsen, P.; Hrdlicka, P. J. *J. Org. Chem.* **2011**, *76*, 7119−7131. (b) Didion, B. A.; Karmakar, S.; Guenther, D. C.; Sau, S.; Verstegen, J. P.; Hrdlicka, P. J. *ChemBioChem* **2013**, *14*, 1534−1538. (c) Denn, B.; Karmakar, S.; Guenther, D. C.; Hrdlicka, P. J. *Chem. Commun.* **2013**, *49*, 9851−9853.

(9) (a) Kumar, T. S.; Madsen, A. S.; Wengel, J.; Hrdlicka, P. J. *J. Org. Chem.* **2006**, *71*, 4188−4201. (b) Kumar, T. S.; Madsen, A. S.; Østergaard, M. E.; Sau, S. P.; Wengel, J.; Hrdlicka, P. J. *J. Org. Chem.* **2009**, *74*, 1070−1081.

(10) Kumar, T. S.; Wengel, J.; Hrdlicka, P. J. *ChemBioChem* **2007**, *8*, 1122−1125.

(11) Kumar, T. S.; Madsen, A. S.; Østergaard, M. E.; Wengel, J.; Hrdlicka, P. J. *J. Org. Chem.* **2008**, *73*, 7060−7066.

(12) (a) Sau, S. P.; Kumar, T. S.; Hrdlicka, P. J. *Org. Biomol. Chem.* **2010**, *8*, 2028−2036. (b) Sau, S. P.; Madsen, A. S.; Podbevsek, P.; Andersen, N. K.; Kumar, T. S.; Andersen, S.; Rathje, R. L.; Anderson, B. A.; Guenther, D. C.; Karmakar, S.; Kumar, P.; Plavec, J.; Wengel, J.; Hrdlicka, P. J. *J. Org. Chem.* **2013**, *78*, 9560−9570.

(13) A conference proceeding outlining a portion of this study has been published. See: Andersen, N. K.; Wengel, J.; Hrdlicka, P. J. *Nucleosides, Nucleotides Nucleic Acids* **2007**, *26*, 1415−1417.

(14) Wenska, M.; Honcharenko, D.; Pathmasiri, W.; Chattopadhyaya, J. *Heterocycles* **2007**, *73*, 303−324.

(15) Rosenbohm, C.; Christensen, S. M.; Sørensen, M. D.; Pedersen, D. S.; Larsen, L.-E.; Wengel, J.; Koch, T. *Org. Biomol. Chem.* **2003**, *1*, 655−663.

(16) Hrdlicka, P. J.; Andersen, N. K.; Jepsen, J. S.; Hansen, F. G.; Haselmann, K. F.; Nielsen, C.; Wengel, J. *Bioorg. Med. Chem.* **2005**, *77*, 2597−2621.

(17) (a) Ellervik, U.; Magnusson, G. *Tetrahedron Lett.* **1997**, *38*, 1627−1628. (b) Rigoli, J. W.; Østergaard, M. E.; Canady, K. M.; Guenther, D. C.; Hrdlicka, P. J. *Tetrahedron Lett.* **2009**, *50*, 1751−1753.

(18) The conversion of **7** into **9** has been outlined in the patent literature. See: Sørensen, M. D.; Wengel, J.; Koch, T.; Christensen, S. M.; Rosenbohm, C.; Pedersen, D. S. WO 2003095467 A1.

(19) Takaku, H.; Morita, K.; Sumiuchi, T. *Chem. Lett.* **1983**, 1661−1664.

(20) The signal for H3′ appears as a doublet in nucleosides with unmodified 3′-OH groups.

(21) Abdel-Magid, A. F.; Carson, K. G.; Harris, B. D.; Maryanoff, C. A.; Shah, R. D. *J. Org. Chem.* **1996**, *61*, 3849−3862.

(22) Hakånsson, A. E.; Wengel, J. *Bioorg. Med. Chem. Lett.* **2001**, *11*, 935−938.

(23) Crothers, D. M. *Biopolymers* **1968**, *6*, 575−584.

(24) (a) Yamana, K.; Iwase, R.; Furutani, S.; Tsuchida, H.; Zako, H.; Yamaoka, T.; Murakami, A. *Nucleic Acids Res.* **1999**, *27*, 2387−2392. (b) Christensen, U. B.; Pedersen, E. B. *Nucleic Acids Res.* **2002**, *30*, 4918−4925. (c) Bryld, T.; Højland, T.; Wengel, J. *Chem. Commun.* **2004**, 1064−1065.

(25) Marin, V.; Hansen, H. F.; Koch, T. R.; Armitage, B. A. *J. Biomol. Struct. Dyn.* **2004**, *21*, 841−850.

(26) (a) Korshun, V. A.; Stetsenko, D. A.; Gait, M. J. *J. Chem. Soc., Perkin Trans. 1* **2002**, 1092−1104. (b) Dohno, C.; Saito, I. *ChemBioChem* **2005**, *6*, 1075−1081.

(27) (a) Dougherty, G.; Pilbrow, J. R. *Int. J. Biochem.* **1984**, *16*, 1179−1192. (b) Nakamura, M.; Fukunaga, Y.; Sasa, K.; Ohtoshi, Y.; Kanaori, K.; Hayashi, H.; Nakano, H.; Yamana, K. *Nucleic Acids Res.* **2005**, *33*, 5887−5895. (c) Asanuma, H.; Fujii, T.; Kato, T.; Kashida, H. *J. Photochem. Photobiol., C* **2012**, *13*, 124−135.

(28) (a) Okamoto, A.; Kanatani, K.; Saito, I. *J. Am. Chem. Soc.* **2004**, *126*, 4820−4827. (b) Østergaard, M. E.; Kumar, P.; Baral, B.; Guenther, D. C.; Anderson, B. A.; Ytreberg, F. M.; Deobald, L.; Paszczynski, A. J.; Sharma, P. K.; Hrdlicka, P. J. *Chem.—Eur. J.* **2011**, *17*, 3157−3165.

(29) Manoharan, M.; Tivel, K. L.; Zhao, M.; Nafisi, K.; Netzel, T. L. *J. Phys. Chem.* **1995**, *99*, 17461−17472. (b) Seo, Y. J.; Ryu, J. H.; Kim, B. H. *Org. Lett.* **2005**, *7*, 4931−4933.

(30) Persil, O.; Hud, N. V. *Trends Biotechnol.* **2007**, *25*, 433−436.

(31) The assignments of the $^{1}$H NMR signals (and of the corresponding $^{13}$C signals) of H5′, H5″, and $CH_2$Ph (if present) are interchangeable.

(32) The least predominant rotamer is denoted as “A”.